Exposure to negative socio-emotional events induces sustained alteration of resting-state brain networks in the elderly

Sebastian Baez Lugo (sebastian.baezlugo@unige.ch)
University of Geneva https://orcid.org/0000-0002-7781-2387
Yacila Deza-Araujo
University Of Geneva https://orcid.org/0000-0002-2624-077X
Fabienne Collette
University of Liège https://orcid.org/0000-0001-9288-9756
Patrik Vuilleumier
Lab NIC https://orcid.org/0000-0002-8198-9214
Olga Klimecki
University of Geneva https://orcid.org/0000-0003-0757-7761
and The Medit-Ageing Research group

Research Article

Keywords: Ageing, Anxiety, Rumination, Emotional resilience, Default Mode Network, Functional connectivity, Amygdala, Insula, Posterior cingulate cortex, fMRI

Posted Date: November 3rd, 2020

DOI: https://doi.org/10.21203/rs.3.rs-91196/v2

Title:

Exposure to negative socio-emotional events induces sustained alteration of resting-state brain networks in the elderly

Authors:

Sebastian Baez Lugo[1,2,*], Yacila I. Deza-Araujo[1,2], Fabienne Collette[3], Patrik Vuilleumier[1,2], Olga Klimecki[1,4], and the Medit-Ageing Research Group

Affiliations:

[1] Swiss Center for Affective Sciences, University of Geneva, Geneva, Switzerland.

[2] Laboratory for Behavioral Neurology and Imaging of Cognition, Department of Neuroscience, Medical School, University of Geneva, Geneva, Switzerland.

[3] GIGA-CRC In Vivo Imaging Research Unit, University of Liège, Liège, Belgium.

[4] Psychology Department, Technische Universität Dresden, Dresden, Germany.

* Correspondence concerning this article should be addressed to: **sebastian.baezlugo@unige.ch**

Abstract:

Socio-emotional functions seem well-preserved in the elderly. However, the long-lasting effects that the exposure to others' distress may provoke in the brain remain unknown in this population. To evaluate how the aging brain reacts during and after emotionally challenging social events, we designed a new "task-rest" paradigm in which elderly participants (*N*=127) underwent functional magnetic resonance imaging (fMRI) while exposed to socio-emotional videos. We unveil neural markers of "emotional inertia" in brain activity and connectivity following negative scenes. Exposure to others' suffering induced differential activations that lingered over time into the subsequent resting-state in regions of the default mode network (DMN). Moreover, emotional elicitation potentiated subsequent resting-state connectivity between posterior DMN and amygdala, which in turn was related to anxiety, rumination, and negative thoughts. These findings uncover brain mechanisms underlying emotional resilience and empathy in the elderly and may help understand how poor social stress regulation promotes neurodegenerative diseases.

Keywords:

Ageing, Anxiety, Rumination, Emotional resilience, Default Mode Network, Functional connectivity, Amygdala, Insula, Posterior cingulate cortex, fMRI.

INTRODUCTION

Aging is a multifaceted process associated with many changes in bodily and mental health. While there is a general decline in physical performances and cognitive abilities in aging [1], emotional functions appear to be maintained or even enhanced in older adults relative to younger adults [2–4]. Indeed, the elderly tend to regulate their emotional states well, a crucial capacity for affective well-being and healthy aging [5]. Unlike younger adults, they often prioritize social and emotional interactions over other goals [6] and show a "positivity bias" in emotion perception [7]. In contrast, maladaptive emotional reactivity and impaired emotion regulation are related to affective psychopathologies such as anxiety, depression, worry, and rumination throughout the lifespan [8,9], including in aging [10]. There is also growing evidence that maladaptive affective styles may represent a significant risk factor for dementia [11–14], one of the primary mental health burdens in the elderly population [15]. However, the neural substrates underpinning proficient socio-affective processing and emotional resilience in the elderly remain unresolved and still scarcely investigated.

An important marker of maladaptive affective style is "emotional inertia", which denotes the degree to which emotions carry over from one moment to the next [16]. Emotional inertia may reflect unsuccessful recovery mechanisms following the offset of affective events and low resilience to stress, associated with higher risks of depression [17,18] and higher trait anxiety and rumination tendencies [19]. Most studies of emotional inertia employed behavioral measures based on experience sampling methods [16,20], e.g., requiring participants to report their affective state at different time points and measuring autocorrelations between successive time-points or events [16,21,22]. More recently, a few neuroimaging studies investigated emotional inertia at the brain level using “task-rest” paradigms [23–29], in which brain activity during rest at time T is probed as a function of different task-induced activations at time T-1 [30]. For example, positive or negative emotions evoked by images or videos were found to induce carryover effects on brain activity and/or connectivity during subsequent resting-state in default mode and affective networks [24,28]. These carryover effects have been observed at different time scales ranging from a few seconds [31] to several minutes [27], following different task instructions ranging from passive viewing through to active regulation of emotions [23], and across different conditions of emotional valence and intensity [25,26].

At the neural level, most brain imaging studies found carryover effects of emotions on the functional dynamics of the default mode network (DMN) either in the form of increased [26,31] or decreased [24,25] activity patterns in regions comprising the medial prefrontal cortex (MPFC), posterior cingulate cortex (PCC), precuneus, and inferior parietal cortex. These regions of the DMN

are usually active when individuals are free to let their mind wander in undisturbed conditions [32,33]. Similar effects have also been observed in the insula and amygdala [24]; two regions critically involved in emotional and social processing [34–36]. For instance, a slow recovery of amygdala activity (i.e., longer return to baseline level) after negative images was reported in individuals with higher neuroticism [37]. Slower recovery of amygdala activity after emotional videos was furthermore associated with higher anxiety traits and ruminations [19]. Subcortical limbic regions such as the amygdala and striatum also display sustained changes in their functional connectivity with cortical areas in medial PFC and PCC during rest after negative emotions [24] and reward [28]. These findings converge with other studies showing that disturbances in functional connectivity of the amygdala with medial parts of the DMN at rest are associated with anxiety (e.g., decreased connectivity with MPFC [38]) and mood disorders (e.g., increased connectivity with PCC [39]). Taken together, these data suggest that long-lasting carryover effects of emotions on activity and connectivity of limbic networks may provide an important neural marker of emotional regulation style and affective resilience.

Yet, all previous neuroimaging studies of emotional carryover focused on young healthy participants. It remains unknown whether emotional inertia also occurs in the elderly population, how it is modified given the well-known "positivity bias" observed in the elderly [2,3], and which brain networks are involved. Here we therefore used a similar task-rest paradigm to probe for carryover effects in a large sample of healthy elderly participants, and identify neural substrates of individual differences in emotional inertia in this population. Defining valid markers of adaptive emotion regulation abilities in a naturalistic paradigm, without making high cognitive demands required by more voluntary/explicit regulation strategies [40], would be valuable to better understand affective resilience mechanisms and better predict affective risk factors associated with pathological aging and dementia [14].

In addition, previous work did not assess whether emotional inertia is modulated by individual differences in empathy, which may strongly influence how people react to negative socio-affective stimuli presented in neuroimaging studies [19,24], and thus how they recover from induced emotions [27]. Because social competences and affective empathy are relatively preserved in the elderly [4], socially significant emotional events offer an optimal window to probe emotional reactivity and regulation in this population. Moreover, there is only scarce research on empathy in older people [4,41–43]. Behaviorally, cognitive empathy declines in older compared to younger people, while affective empathy may remain intact or even improve [4]. At the brain level, hemodynamic responses to the perception of others' pain were reported to be reduced in anterior insula (AI) and cingulate cortex (ACC) [41]; two regions implicated in pain processing, negative affect, and salience

detection [35,44]. However, despite the importance of social interactions and emotional resilience for healthy aging [45–47], the neural underpinnings of (mal)adaptive affective reactivity as well as their link with individual empathic skills and personality traits have not been investigated during aging yet.

To address these issues, we designed a novel "task-rest" paradigm combining two lines of research: short (10-18s) empathy inducing videos from the Socio-affective Video Task (SoVT) [48] were shown interspersed with rest periods of 90 seconds (similar to Eryilmaz and colleagues [24]) while participants underwent functional magnetic resonance imaging (fMRI) of brain activity. The SoVT videos consisted of short silent scenes depicting suffering people (high emotion videos) or people in everyday life situations (low emotion videos). By adding short resting state periods after blocks of videos of each kind, the SoVT-Rest allowed us to evaluate how the aging brain reacts both during and after exposure to emotionally challenging social information. In addition, we assessed whether emotional inertia in brain networks is modulated by empathic traits and anxiety, and how it relates to rumination tendencies. We hypothesized that exposure to others' suffering (relative to neutral social situations) would (1) engage brain regions implicated in emotional saliency and empathy (i.e., insula, aMCC), (2) induce subsequent carryover effects in functional connectivity at rest between these regions and the DMN, and (3) unveil neural markers of maladaptive emotional recovery that should be associated with anxiety, ruminative thinking, and negative emotions.

Material and Methods

Participants

A total of 135 healthy elderly participants with corrected-to-normal vision and no history of neurological or psychiatric disorders, aged between 65 and 83 years, took part in our study. This session was part of the baseline visit of the Age-Well randomized clinical trial within the Medit-Ageing Project [49]. Detailed inclusion criteria of the Age-Well randomized clinical trial are provided in Supplementary Table 1. Participants were recruited via advertising in media outlets, social media, and flyers distributed in relevant local events and places. A total of 8 participants were excluded from final data analysis due to the following a priori exclusion criteria: abnormal brain morphology (n = 3), extreme head motion (n = 3), and presence of artifacts in brain images (n = 2). The final sample for the current study included 127 participants (M age = 68.8 years, SD = 3.63, 79 females. See Table 1 for participants' characteristics). This sample size was sensitive enough to detect small-to-medium-sized effects at a voxel level (α = 0.001, dz = 0.37), given a power of 1-β = 0.8 [50]. All

participants provided written informed consent prior to participation. The Age-Well randomized clinical trial was approved by the ethics committee (Comité de Protection des Personnes Nord-Ouest III, Caen, France; trial registration number: EudraCT: 2016-002441-36; IDRCB: 2016-A01767-44; ClinicalTrials.gov Identifier: NCT02977819).

Questionnaires

In order to account for inter-individual differences in psycho-emotional profile, participants filled in different questionnaires assessing personality traits and cognitive functions, including empathy (Interpersonal Reactivity Index, IRI [51]), depression (Geriatric Depression Score, GDS [52]), anxiety (STAI-trait Anxiety Index, STAI [53]), emotion regulation capacities (Emotion Regulation Questionnaire, ERQ [54]), and rumination levels (Rumination Response Scale, RRS [55]). The summary of these questionnaires is provided in Table 1. All scores were in the normative range. For a full list of tasks and measures used in the Age-Well trial, please refer to Poisnel and colleagues [49].

Table 1. Participant characteristics

		n	Min	Max	Mean	Std. Dev
Demographics						
Sex	Female	79				
	Male	48				
Age		127	65	83	68.81	3.63
Education (n. of years)		127	7	22	13.21	3.1
Personality traits and Cognitive functions						
STAI	Trait	127	20	54	34.57	7.12
Rumination Response Scale	Total	126	22	68	35.67	8.55
	Reflection	126	5	17	8.93	3.23
	Brooding	126	5	16	8.06	2.28
Interpersonal Reactivity Index	Distress	127	0	26	10.18	5.27
	Empathic Concern	127	8	28	19.76	4.18
	Perspective Taking	127	9	28	17.50	3.56
	Fantasy	127	1	28	14.35	4.75
Emotion regulation abilities	Reappraisal	127	6	40	29.61	5.79
	Suppresion	127	4	28	16.54	5.19
Geriatric Depression Scale	Global	127	0	11	1.31	1.77

n, number of participants; Std Dev, Standard deviation.

Socio-affective Video Task-Rest (SoVT-Rest)

The emotion-elicitation task used in this study is adapted from the previously validated Socio-affective Video Task (SoVT) [48,56]. The SoVT aims at assessing social emotions (e.g., empathy) in response to short silent videos (10-18s). During this task, participants watch 12 High Emotion (HE) and 12 Low Emotion (LE) video-clips grouped in blocks of three. HE videos depict suffering people (e.g., due to injuries or natural disasters), while LE videos depict people during everyday activities (e.g., walking or talking). In this study, each block was followed by a resting state period of 90 seconds in order to assess the carryover effects of emotion elicitation on subsequent resting-state brain activity (similar to Eryilmaz and colleagues [24]). This combination of both paradigms (task and

rest) was specifically designed to test for emotional inertia and its relation to empathy. The combined task (called SoVT-Rest) is illustrated in Fig. 1.

Overall, three sets (V1, V2, and V3) of 24 videos each were created and randomized across participants. In the final sample, n = 42 participants thus saw the video set V1, n = 40 video set V2, and n = 45 video set V3. During the SoVT-Rest, these videos were presented in two separate runs, with each run followed by a thought probe to assess current mental content during the last rest period (after LE videos in one run and after HE videos in the other run). The order in which runs were presented was randomized so that half of the participants started the experiment with a HE block and the other half with an LE block. The total duration of the SoVT-Rest fMRI paradigm was approximately 21 minutes, consisting of 9.5 min for each run plus 1 minute on average for each thought probe.

After the fMRI session, participants watched all video clips again on a computer outside the scanner and provided ratings on their subjective experience of empathy ("To what degree did you feel the emotions of the characters?") as well as their subjective positive affect ("Indicate the intensity of your positive emotions") and negative affect state ("Indicate the intensity of your negative emotions") (translated from French), for each of the 24 videos. Each scale offered 21 possible responses ranging from 0 ("Not at all") to 10 ("Extremely") with increments of 0.5. The order of questions was always the same: empathy, positive affect, and negative affect. The total time for the out-of-scanner rating session was, on average, 10 minutes. Onset times and response times for both neuroimaging and behavioral tasks were collected via the Cogent toolbox (developed by Cogent 2000 and Cogent Graphics) implemented in Matlab 2012 (Mathworks Inc., Natick, MA, USA).

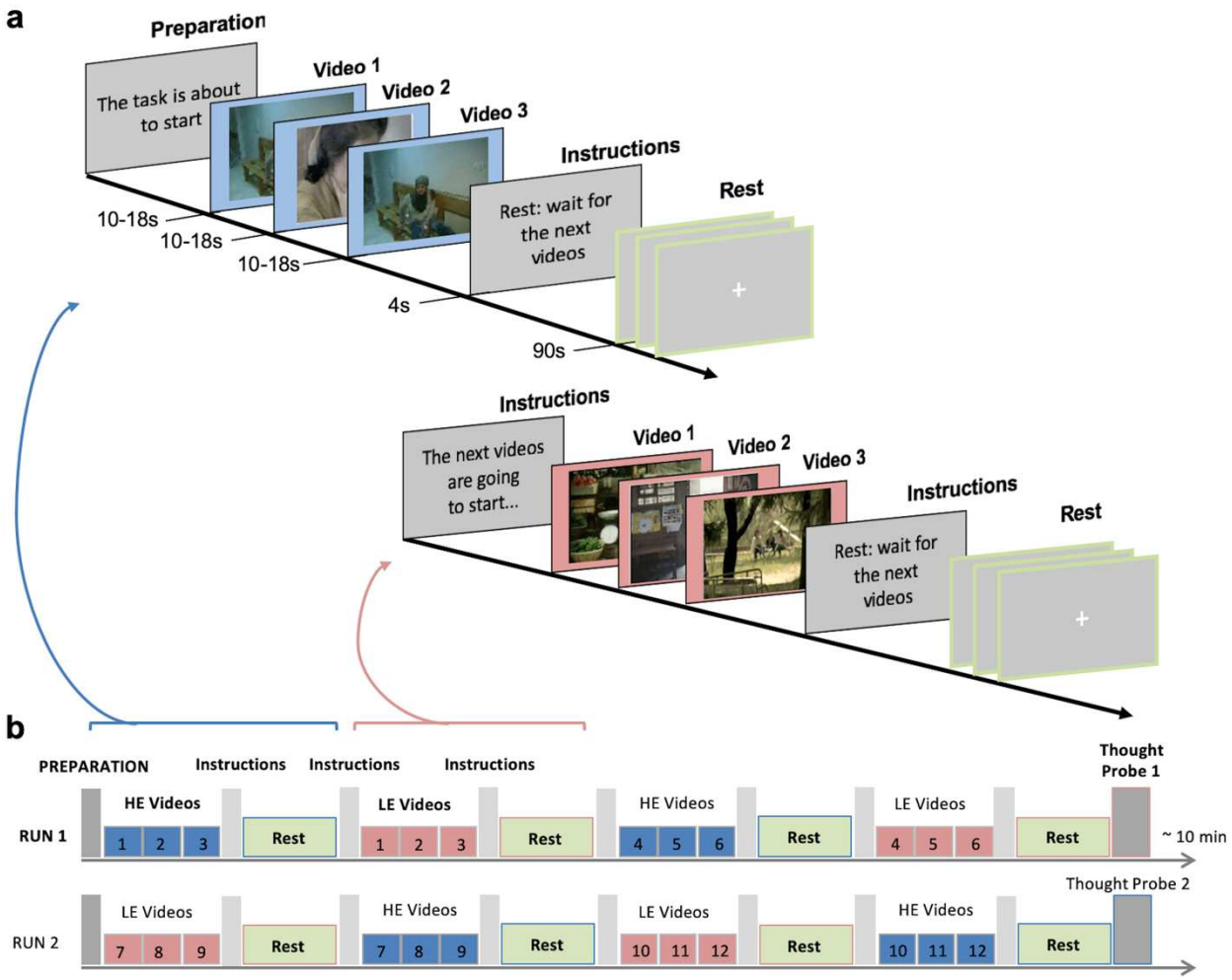

Figure 1. Experimental design: (**a**) SoVT-Rest paradigm: 12 **High Emotion (HE)** and 12 **Low Emotion (LE)** videos were presented grouped in blocks of three. HE videos depict suffering people (e.g., due to injuries or natural disasters), while LE videos depict people during everyday activities (e.g., walking or talking). Each block of three videos is followed by a resting state period of 90 seconds. (**b**) Each run ends with a thought probe in which participants verbally express what they had been thinking and/or feeling during the last rest period (via a microphone), once following a LE block and once following a HE block. The order of the runs was randomized between participants.

Behavioral data analysis.

We performed a repeated measures multivariate analysis of variance (MANOVA, with Pillai's trace statistics) with the within-subject factor "video type" (HE and LE), the between-subject factor "video set" (V1, V2, V3), and three dependent variables: ratings of empathy, positive affect, and negative affect. This was followed up by pairwise *t*-tests. We also computed Spearman's rank correlations between these different scores. Additionally, we performed correlation analyses between the ratings of empathy, positive affect, and negative affect of videos and the relevant personality traits measured by the above-mentioned questionnaires, using non-parametric

Spearman's rank correlations because some of these variables were not normally distributed. All statistical analyses are reported with a significance level of $p < 0.05$, and when necessary, *p*-values are corrected for multiple comparisons using the False Discovery Rate (FDR) method [57]. The statistical analyses were performed with R studio (version 3.6.1) and the corresponding graphs were created with ggplot2 (version 3.2.1).

Acquisition and preprocessing of MRI data.

Magnetic Resonance Imaging (MRI) scans were acquired at the GIP Cyceron (Caen, France) using a Philips Achieva (Eindhoven, The Netherlands) 3T scanner with a 32-channel head coil. Participants were provided with earplugs to protect hearing and their heads were stabilized with foam pads to minimize head motion. A high-resolution T1-weighted anatomical volume was first acquired using a 3D fast field echo sequence (3D-T1-FFE sagittal; repetition time = 7.1 ms; echo time = 3.3 ms; flip angle = 6°; 180 slices with no gap; slice thickness = 1 mm; field of view = 256x256 mm^2; in plane resolution = 1x1 mm^2). Blood oxygen level-dependent (BOLD) images were acquired during the SoVT-Rest task with a T2*-weighted asymmetric spin-echo echo-planar sequence (each run ~10.5 min; TR = 2000 ms, TE = 30 ms, flip angle = 85°, FOV = 240 x 240 mm^2, matrix size = 80 x 68 x 33, voxel size = 3 × 3× 3 mm^3, slice gap = 0.6 mm) in the axial plane parallel to the anterior-posterior commissure. During each functional run, about 310 contiguous axial images were acquired and the first two images were discarded because of saturation effects. Additionally, in order to improve the preprocessing and enhance the quality of the BOLD images [58], T2 and T2* structural volumes were collected. Each functional and anatomical image was visually inspected to discard susceptibility artifacts and anatomical abnormalities.

Quality control and preprocessing were conducted using Statistical Parametric Mapping software (SPM12; Wellcome Trust Centre for Neuroimaging, London, United Kingdom) on Matlab 2017 (Mathworks Inc., Natick, MA, USA). Prior to the preprocessing, we manually centered the images to the AC-PC axis, realigned the functional and anatomical MRI images and then realigned all images to the last version of the SPM anatomical template "ch2". The preprocessing procedure was done with SPM12 and followed a methodology designed to reduce geometric distortion effects induced by the magnetic field, described by Villain and colleagues [58]. This procedure included the following steps: 1) realignment of the EPI volumes to the first volume and creation of the mean EPI volume, 2) coregistration of the mean EPI volume and anatomical T1, T2, and T2* volumes, 3) warping of the mean EPI volume to match the anatomical T2* volume, and application of the deformation parameters to all the EPI volumes, 4) segmentation of the anatomical T1 volume, 5)

normalization of all the EPIs, T1 and T2* volumes into the Montreal Neurological Institute (MNI) space using the parameters obtained during the T1 segmentation, 6) 8 mm FWHM smoothing of the EPI volumes.

For each individual, frame-wise displacement (FD) [59] was calculated. FD values greater than 0.5 mm were flagged to be temporally censored or "scrubbed" during the first-level analysis (see description below). The average of FD volumes censored was M = 6.8 (SD = 8.3, Min = 1 , Max = 38) for both runs for a total of n=65 participants. In addition, other n=3 participants were excluded from further analysis because the number of volumes with FD > 0.5 mm exceeded 10% of the total volumes acquired in one run.

General linear model analysis with SPM

The MRI SoVT-Rest data was analyzed using General Linear Models in SPM12 (implemented in Matlab 2017). This comprised a standard first-level analysis at the subject level, followed by a random effect (2nd-level) analysis to assess the effects of interest at the group level. For the 1st-level analysis, a design matrix consisting of two separate sessions was constructed for each participant. Experimental event regressors in each session included the fixation cross (10 sec), instructions (4 sec), three videos (~15 sec each) modeled separately, and rest periods following each block (90 sec). Each rest period was divided into three equal parts (30 sec time bins), in order to model different time intervals during which brain activity may gradually change after the end of the HE and LE video blocks (similar to Eryilmaz and colleagues [24]).

The different regressors were then convolved with a hemodynamic response function (HRF) according to a block design for univariate regression analysis. The six realignment parameters were added to the matrices in order to account for motion confounds, and low-frequency drifts were removed via a high-pass filter（cutoff frequency at 1/ 256 Hz). The final 1st-level matrix consisted of 2 sessions of 21 regressors each (1 fixation cross + 1 instruction for videos + 1 instructions for rest + 3 HE videos + 3 post HE rest + 3 LE videos + 3 post LE rest + 6 motion parameters). Additionally, to address the influence of remaining motion on BOLD data, we performed data censoring as described by Power and colleagues [59]. Specifically, during the estimation of beta coefficients for each regressor of interest, volumes with FD >0.5 mm were flagged in the design matrices and ignored during the estimation of the 1st -levels.

For the 2nd-level analysis, we used a flexible factorial design where the estimated parameters from 1st-level contrasts of interest were entered separately for each subject. The second-level design matrix was generated with SPM12 and included 12 regressors of interest (3 HE videos

+ 3 Post HE rest + 3 LE videos + 3 Post LE rest). This step allowed us to investigate the effect of each experimental condition on brain activity, including the main condition effects (video and rest) as well as the specific emotional effects (HE and LE) during either the video or the subsequent rest periods.

We then conducted T-tests contrasts to compare the conditions of interest (videos vs. rest periods and vice versa) as well as the specific emotional effects (videos: HE vs. LE; rest: HE vs. LE). We also identified voxels that were most reliably activated for a specific contrast (HE > LE) across the two periods (videos and rest) by applying an inclusive masking from one contrast (e.g., videos: HE > LE) to the other contrast (rest: HE > LE) with a strict threshold used for both ($p < 0.00001$). All comparisons are reported with a whole-brain family-wise error (FWE) correction at $p < 0.05$, at the voxel level.

Functional connectivity analysis during rest periods, definition of Regions of Interest (ROI), and the data analysis pipeline

We conducted functional connectivity analyses between the most important brain regions of interest (ROIs) associated with the empathy network and with the default mode network (DMN). In addition, we also included the bilateral amygdalae among regions used for this analysis, because previous studies assessing carryover effects in the brain have related sustained amygdala activity to anxiety traits [19] and emotional reactivity [37]. For nodes of the DMN, we choose the posterior cingulate cortex (PCC) and the anterior medial prefrontal cortex (aMPFC), following Andrews-Hanna and colleagues [60]. Based on the results of a meta-analysis by Fan and colleagues [44], the bilateral anterior insula (AI) and anterior medial cingulate cortex (aMCC) were used as ROIs in the empathy network. Time-series were extracted from 6 mm-radius spheres around the peak of each of these ROIs. The amygdala was defined anatomically using the current SPM anatomical template provided by Neuromorphometrics, Inc (http://Neuromorphometrics.com/).

Functional connectivity analyses were performed using Matlab 2017 and R studio (version 3.6.1). For each participant, time courses of activity (from each voxel of the brain) were high-pass filtered at 256 Hz, detrended and standardized (Z-score), before extracting specific time courses from the defined ROIs. Nuisance regressors included white matter (WM) and cerebrospinal fluid (CSF) signals, and the realignment parameters. For each participant, time-series from the instructions and videos periods were removed, and the remaining time series corresponding to the rest periods were concatenated. This procedure was previously proposed by Fair and colleagues [61] and proved to be qualitatively and quantitatively very similar to continuous resting-state data.

Additionally, in order to correct extreme head motion without affecting the autocorrelation of the time series, image volumes flagged with FD > 0.5mm were removed and replaced by interpolation (every flagged volume X was replaced by the estimated mean of the X-1 and X+1 volumes). The final concatenated time series resulted in 184 frames (~386 s) of resting-state data for each subject.

We then correlated the time-courses between the different ROIs using Pearson correlations [62] and the resulting coefficients were Fisher's *r* to *z* transformed in order to improve normality in the data. Individual *Z*-score maps (correlation matrices) were created for each participant (see Fig. 2a,b,c). To test for significant differences between the two correlation matrices (post HE rest and post LE rest), we used a non-parametric permutation test [63]. For each pair of nodes, the permutation test compared the true correlation difference (e.g., HE - LE) to a null distribution built by randomly flipping the sign of the correlation coefficients and computing the difference many times (n=5000) (see Fig. 2d). More precisely, for each pair of nodes (e.g., HE - LE for ROI 1 and ROI 3), a vector of n=127 values was obtained and a one-sample *t*-test was computed to obtain the real *t* value (t_{real}). Then, the signs of the elements in the vector were randomly flipped (n=5000) and the model was fitted repeatedly once for every flipping. For each fit, a new realization of the *t* statistic was computed so that an empirical distribution of *t* under the null hypothesis was constructed ($t_{permuted}$). From this null distribution, a *p*-value was computed by assessing the probability of the t_{real} to be higher than 95% of the values on the empirical $t_{permuted}$ distribution [63]. Finally, the obtained *p*-values were converted into an equivalent *Z*-score and significant changes were retained for $Z > 1.64$ (equivalent to $p < 0.05$, one-tailed, uncorrected, marked by an asterisk in matrices).

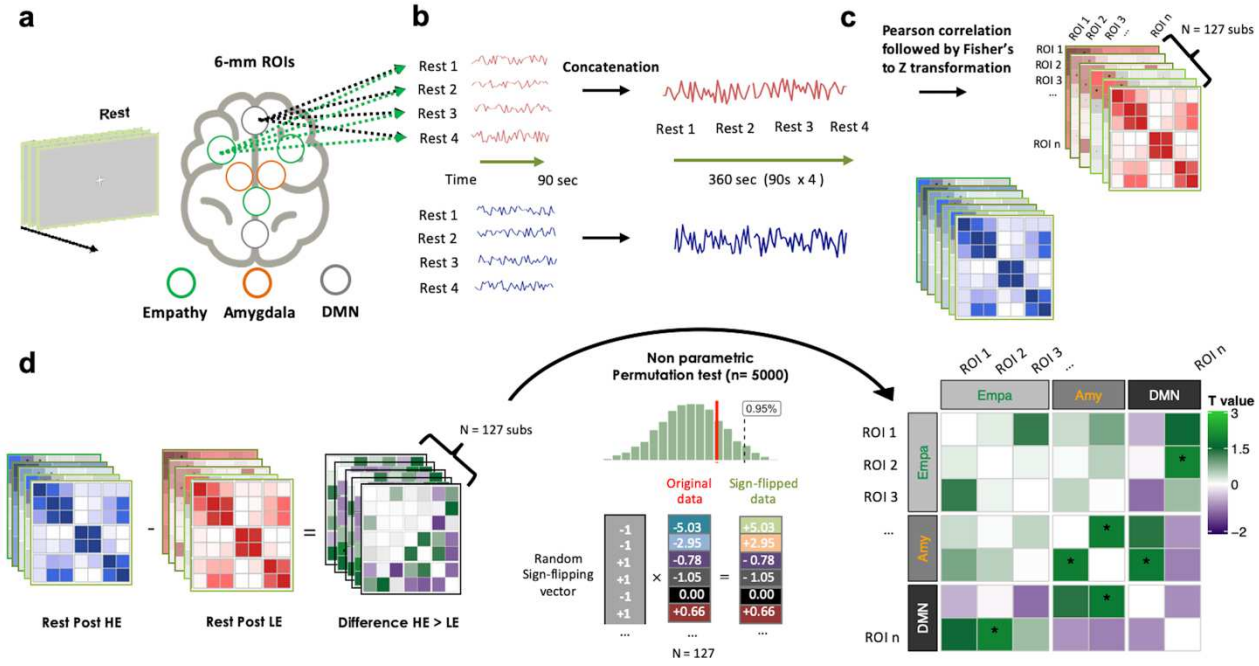

Figure 2. Functional connectivity pipeline: (**a**) Regions of interest (ROIs) from the default mode network (DMN) were chosen based on Andrews-Hanna et al. (2010), including the posterior cingulate cortex (PCC, -8 -56 26) and anterior medial prefrontal cortex (aMPFC, -6 52 -2). ROIs from the empathy network were based on the meta-analysis by Fan et al. (2011), including the bilateral anterior insula (AI, -36 16 2 and 38 24 -2) and anterior mid cingulate cortex (aMCC, -2 24 38). A 6 mm-radius sphere was created for each ROI**.** The amygdala was defined anatomically using the SPM anatomical template. (**b**) For every participant, time-series from the video and instruction periods were removed, and the remaining time series corresponding to the rest periods were concatenated [61]. The final concatenated time series of the four rest blocks for each type of video (high emotion, HE or low emotion, LE) resulted in 184 frames (~360 s) of resting-state data for each subject. (**c**) We then correlated the time-courses between the different ROIs using Pearson's *r* correlation, and the resulting coefficients were Fisher's *r* to *z* transformed to improve normality in the data. Individual *Z*-score maps (correlation matrices) were created for each participant. (**d**) Finally, significant differences between the two correlation matrices (post HE rest vs. post LE rest) were tested using a non-parametric permutation test [63]. For each pair of nodes, the permutation test compared the true correlation difference t_{real} (HE vs. LE) to a null distribution $t_{permuted}$ constructed by randomly flipping the sign of the correlation coefficients and repeating the *t* statistic (*n*=5000).

Thought probes

For each participant, two thought probes were recorded after the last rest period of each run (see Fig. 1b), allowing us to test for differences in spontaneous mind wandering after emotional videos. Following a transcription of the corresponding verbal recordings, the narratives of the participant's responses were analyzed by two independent raters. For each probe (post HE rest and post LE rest),

the raters attributed the presence (Present) or the absence (Absent) of specific thought contents according to a diverse set of pre-defined categories (Supplementary Table 2). These categories were selected according to a priori relevant affective or cognitive dimensions, and included the following: *negative* and *positive emotion*s, *directed attention to oneself* and *to others*, *emotion regulation (voluntary control of emotions)*, *negative* and *positive social emotions, rumination,* and *temporality (present or past/future)*. Categories with low intra-group variability (i.e., less than 15 % in one category) were not included in further analyses (for details, see Supplementary Table 2). The final dimensions included *negative* and *positive emotion*s, *directed attention to oneself* and *to others,* and *positive social emotions*. This final analysis of thought probes comprised data from 109 participants for rest periods after HE videos and 110 participants for the rest periods after LE videos. This was due to i) missing thought probes for 9 participants and ii) exclusion of thought content that did not refer directly to the rest period, but rather to the video for both runs (n = 5), following LE rest (n = 3) or following HE rest (n = 4). Interrater agreement on the final dimensions ranged from 0.28 to 0.66 (Cohen's kappa index; see Supplementary Table 2 for details). The statistical analyses were performed with R studio (version 3.6.1) and the corresponding graphs were created with ggplot2 (version 3.2.1).

Results

Independence of the three parallel video sets of the SoVT-Rest task

To check whether the three video sets elicited similar emotions in this elderly sample, we performed a repeated measures multivariate analysis of variance (MANOVA, with Pillai's trace statistics) with the within-subject factor video type (HE vs LE), the between-subject factor video set (V1, V2, V3), and three dependent variables: empathy, positive affect, and negative affect ratings. As expected, and replicating results from Klimecki and colleagues [48], this analysis revealed no significant differences between the three video sets for any of the self-reported ratings (Pillai's trace = 0.01, $F(1,125) = 0.55$, $p = 0.6$) (see Fig. 3a).

Reliable impact of high compared to low emotion on affective and empathy ratings

We compared the effects of HE and LE videos using pairwise t-tests for each of the three affective ratings (empathy, positive, and negative affect). As predicted, participants reported higher levels of empathy ($t_{126} = 14.5$, $p < 0.001$, $d = 1.31$, two-tailed), higher negative affect ($t_{126} = 26.9$, $p < 0.001$,

d = 2.89, two-tailed), and lower positive affect (t_{126} = -18.9, p < 0.001, d = -2.31, two-tailed), when presented with HE as compared to LE videos (see Fig. 3a). These data validate a successful elicitation of socio-emotional responses with the SoVT-Rest.

Correlation between empathy and affective valence during the SoVT-Rest

To test how empathy was associated with positive and negative affect during HE and LE videos, we computed Spearman correlations between these rating scales. These analyses revealed that during HE videos, empathy correlated positively with negative affect (*rho* = 0.61, p < 0.001) and negatively with positive affect (*rho* = -0.36, p < 0.001). Interestingly, during LE videos, empathy also correlated positively with positive affect (*rho* = 0.62, p < 0.001) but not with negative affect (*rho* = 0.08, p < 0.35) (see Fig. 3b).

Correlation between emotional responses to the SoVT, age, and personality traits

To assess whether levels of empathy, positive affect, and negative affect elicited by the SoVT varied with age and questionnaire measures of empathy, depression, anxiety, rumination and emotion regulation, we conducted additional Spearman rank correlations followed by multiple comparison corrections (using False Discovery Rate). As shown in Figure 3c, this revealed that participants who experienced higher levels of negative emotions during HE videos also reported higher levels of trait anxiety (*rho* = 0.24, p = 0.006) and empathic concern (subscale of the Interpersonal reactivity index; IRI) (*rho* = 0.28, p = 0.001). Empathy during HE videos was also positively correlated with empathic concern on the IRI (*rho* = 0.26, p = 0.002). Interestingly, age was correlated with positive emotions (*rho* = 0.26, p = 0.002) and negatively correlated with negative emotions (*rho* = -0.21, p = 0.01 uncorrected) (see Fig. 3c). For completeness, correlations that did not survive correction for multiple comparisons are also displayed in Fig. 3c.

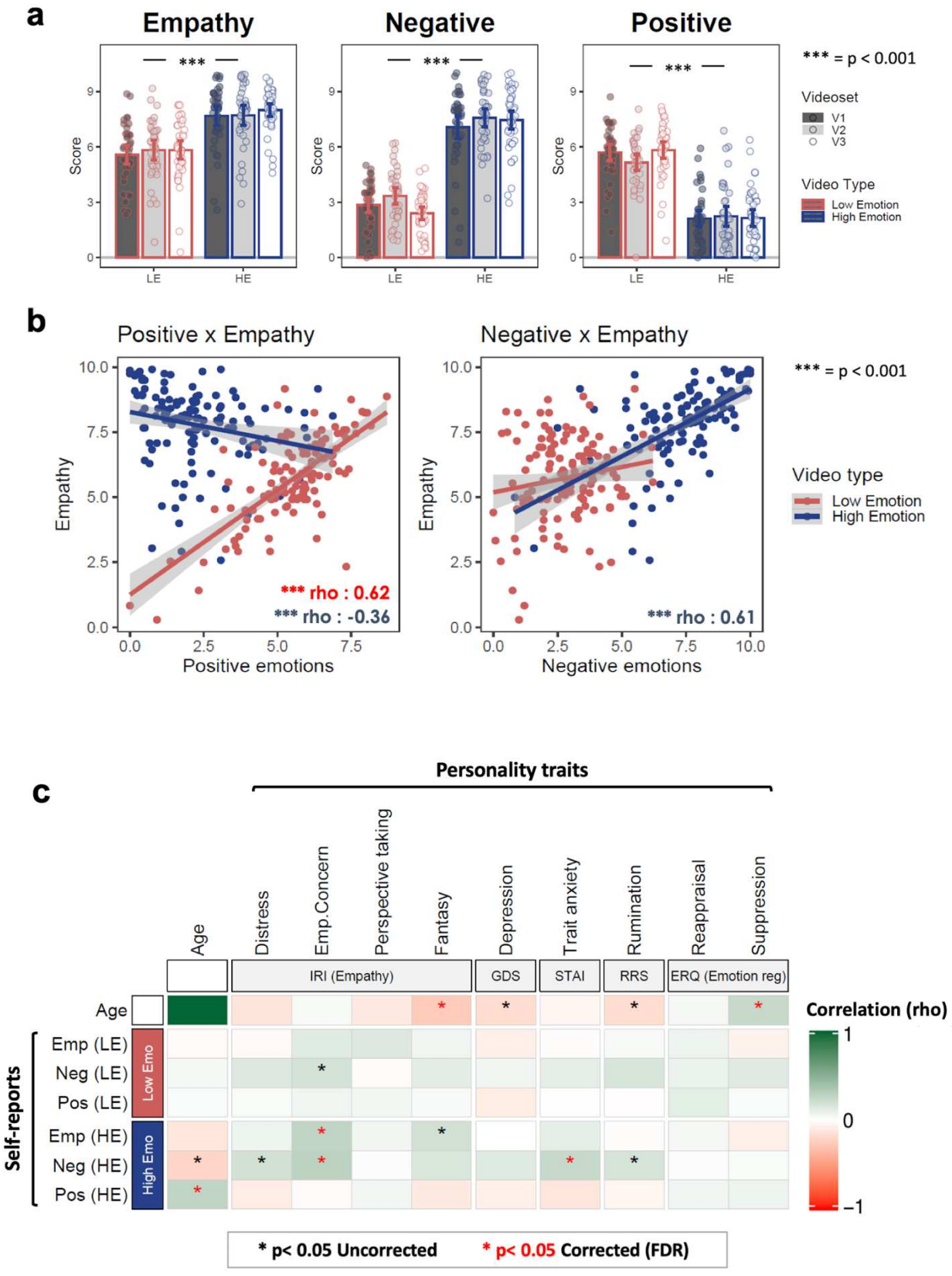

Figure 3. (**a**) Self-reported scores of empathy, positive affect, and negative affect for the HE and LE videos. (**b**) Spearman correlations between self-reported scores of empathy and affective ratings. Error bars represent 95% confidence intervals; dots represent averaged values for each participant per condition, *n* =

127. (**c**) Spearman correlations between age, personality traits, and self-reported scores of empathy, positive affect, and negative affect. Blue: HE videos, Red: LE videos, $n = 126$ (1 missing data point). IRI: Interpersonal Reactivity Index, GDS: Geriatric Depression Score, STAI: STAI-trait Anxiety Index, RRS: Rumination Response Scale, ERQ: Emotion Regulation Questionnaire.

Main effects of videos and rest periods (manipulation check)

Regarding the neuroimaging results, we first verified that the video and rest periods induced differential brain activity by testing for the main effects of task condition. As expected, comparing videos versus rest periods (Videos > Rest, voxel-wise $p < 0.05$ FWE-corrected) revealed greater activity in widespread networks, including strong increases in visual cortices. On the opposite, comparing rest versus video watching periods (Rest > Videos, voxel-wise $p < 0.05$ FWE-corrected) revealed greater activity in several regions typically associated with the default mode network, such as the PCC/Precuneus, ACC/MPFC, and bilateral IPL (see Supplementary Fig. 1 and Supplementary Table 3).

Main brain regions activated when faced with others' suffering during HE videos

We then determined the effect of the emotional content of videos (high vs low). The contrast of HE > LE conditions (voxel-wise $p < 0.05$ FWE-corrected) showed that HE videos (people who are suffering) induced greater activity in several brain areas including bilateral anterior insula (AI), left temporo-parietal junction (l. TPJ), posterior and anterior mid-cingulate cortex (PCC, aMCC), dorsal medial prefrontal cortex (dMPFC), and ventral striatum (VS) (see Fig. 4). These areas overlap with brain networks classically associated with empathy [35,44], compassion [48,56,64], as well as cognitive and affective theory of mind [65,66]. The opposite contrast (LE>HE) showed no significant activation.

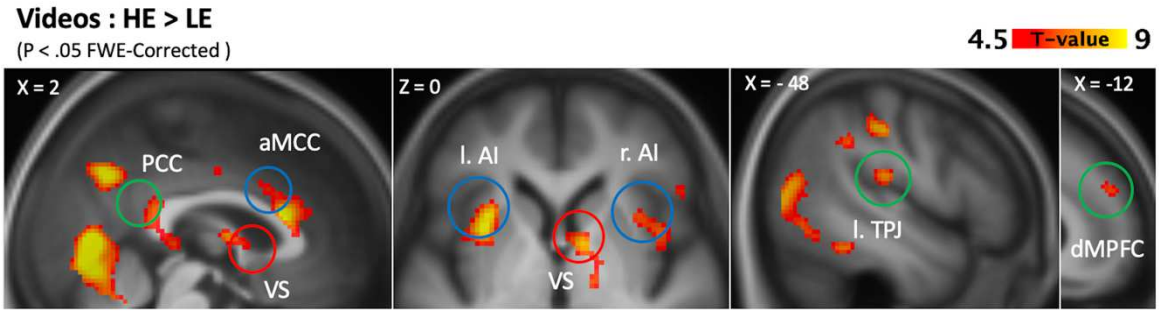

Figure 4. Brain regions with greater activation during high emotion (HE) videos in contrast to low emotion (LE) videos. Reported results are corrected for multiple comparisons using familywise error (FWE) correction at the voxel level (p < 0.05 FWE-corrected). Blue circles show regions previously reported as part of the Empathy network (bilateral anterior insula, AI; anterior middle cingulate cortex, aMCC), green circles show regions previously reported as part of the Theory of Mind network (PCC: posterior cingulate cortex, l. TPJ: left temporo-parietal junction, dMPFC: dorsal medial prefrontal cortex), red circles show regions associated with the Compassion network (VS: ventral striatum) [64,67]. Activations are displayed on the average T1 image of our 127 participants.

Carryover effects of emotional videos observed in the subsequent rest periods:

To test for carryover effects of emotional videos on subsequent resting states [24] and thus assess homeostatic emotion regulation abilities [16], we compared rest periods after HE videos to rest periods after LE videos (post HE > post LE; voxel-wise p < 0.05 FWE-corrected). This contrast revealed greater brain activations in two main areas among the midline nodes of the DMN (ACC/MPFC, and Precuneus/PCC), as well as greater activations of the right amygdala (r.AMY) and the ventral part of the right anterior insula (r.AI) (see Fig. 5a). This accords with previous evidence of emotional inertia effects on brain activity and DMN in younger adults [24].

We then asked whether these carryover effects directly resulted from higher activity in these regions during HE videos. To this aim, we use a masking procedure (see Methods) to overlap the emotional increases (contrasts HE>LE) from both the videos and the rest periods and determine common areas of activity, shared across the task conditions (Fig. 5a). This comparison revealed a restricted overlap in a few selective regions, mainly dMPFC and PCC, where voxels with emotional activation during videos also exhibited emotional carryover effects at rest after videos, suggesting sustained increases persisting over time (Fig. 5c,d). In contrast, other regions differentially activated during emotional videos did not display any carryover effects during the subsequent rest periods (i.e., exclusively responding to HE > LE conditions during the videos periods), including not only

visual cortical areas but also mid cingulate areas (MCC; Fig. 5b). Interestingly the right amygdala as well as a segment of the right anterior insula (ventral part) did not show significant differences for the HE > LE contrast during videos but were robustly activated in the post HE > post LE rest periods (Fig. 5e,f). These dissociations between rest and video-related activity are further illustrated by plots of brain activity (contrasts estimates) over time across the different task periods (using a single time bin of ~45 sec during videos and three successive time bins of 30 seconds during rest to depict the time course of the activation) and the different conditions (HE and LE videos) (Fig. 5).

The opposite contrast (post LE > post HE; voxel-wise $p < 0.05$ FWE-corrected) revealed increased activations in regions including the left parahippocampal gyrus (l.PHG) and the right superior/middle frontal gyrus (r.SFG) (see Supplementary Fig. 2 and Supplementary Table 3). These regions have been previously associated with environmental scenes processing [68], spatial navigation [69], and working memory [70].

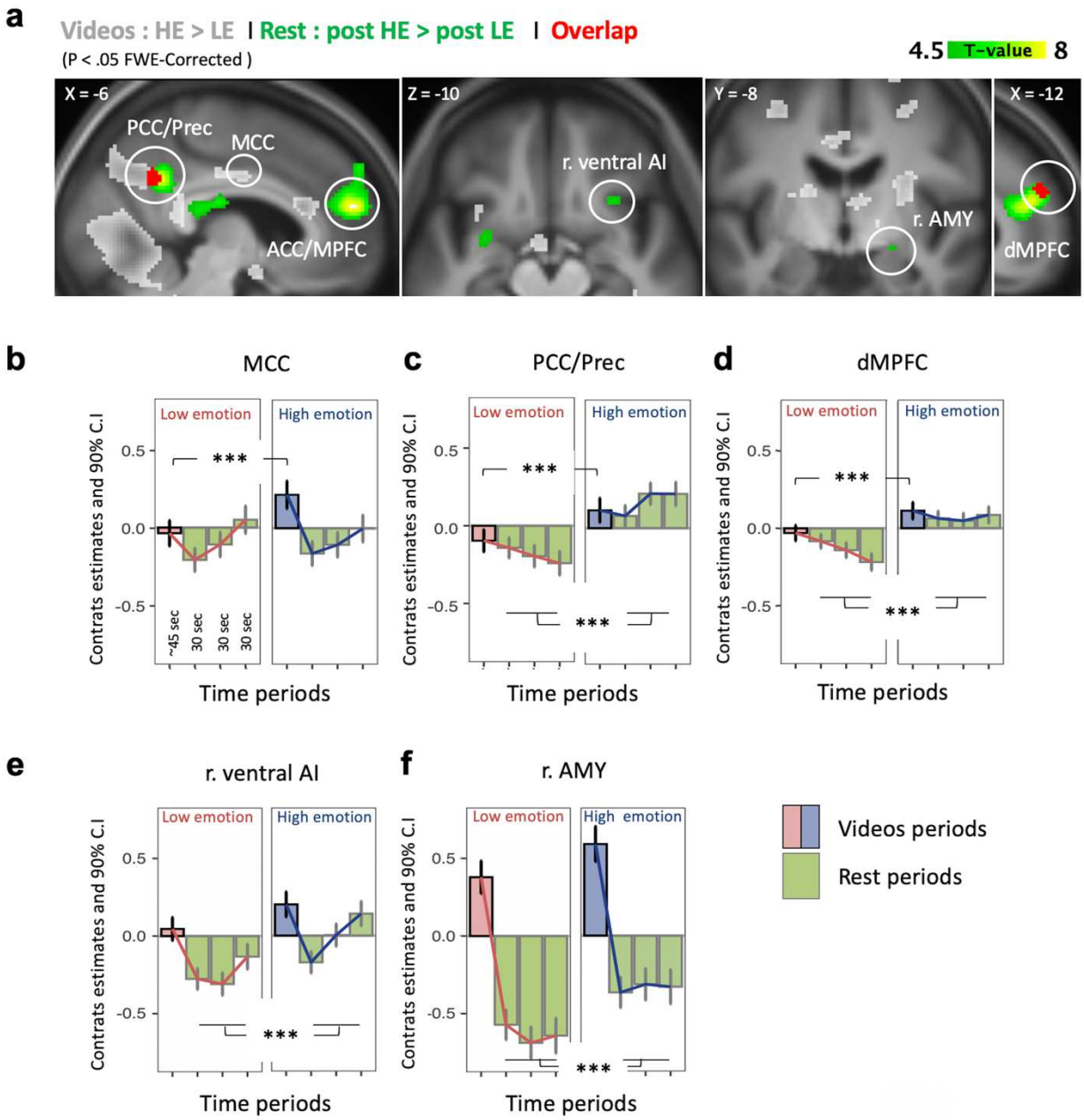

Figure 5. Brain activations to high emotion (HE) versus low emotion (LE) videos and corresponding carryover effects during rest periods. (**a**) Clusters in grey show brain regions significantly activated in the contrast HE videos > LE videos. Clusters in green show brain regions significantly activated in the rest periods corresponding to the contrast post HE videos > post LE videos. Red clusters show the overlap. Reported results are $p < 0.05$ corrected for multiple comparisons using family-wise error (FWE) correction at the voxel level. (**b,c,d,e,f**) Magnitude and time-course of brain activity (parameter estimates) for relevant regions during the different task periods. (**b**) Example of a region (in MCC) responding to HE vs LE videos, but showing no significant difference in activation during rest after HE vs LE videos. (**c,d**) Example of regions (PCC/Prec and dMPFC) responding to HE > LE videos and showing significant carryover with sustained activity during subsequent rest. (**e,f**) The right amygdala as well as the ventral part of the right anterior insula did not reliably respond to HE vs LE videos but showed significant increases in activations during

corresponding rest. Pink lines track activity time-courses during LE conditions, blue lines track activity time-courses during HE conditions. Pink and blue bars indicate activity (blocks of 3 videos = ~45 seconds) for LE and HE videos respectively, green bars indicate activity (over 3 bins of 30 seconds) during rest periods subsequent to corresponding videos periods. Activations are displayed on the average T1 image of our 127 participants. *** $p < 0.05$ FWE-corrected. PCC: posterior cingulate cortex, Prec: precuneus, MCC: mid-cingulate cortex, ACC: anterior cingulate cortex, MPFC: medial prefrontal cortex, dMPFC: dorsal medial prefrontal cortex, r. ventral AI: right anterior insula (ventral part), r. AMY: right amygdala.

Exposure to others suffering impacts subsequent brain network connectivity

To further assess the lingering impact of emotional videos on brain activity dynamics (emotional inertia), we then examined differences in functional connectivity between and within a priori defined networks. To do so, we first determined the functional connectivity patterns in regional time-series from the default mode network, the empathy network, and bilateral amygdala measured during the rest periods after HE videos, compared to the rest periods after LE videos (Fig. 2). We computed connectivity matrices using Pearson correlations between the time-series of every pair of nodes in the three networks of interest. The resulting connectivity matrices obtained for each participant were then group-averaged for illustration (see Fig. 6a).

These brain connectivity maps revealed a general intra-network connectivity (Emp-Emp, Amy-Amy, DMN-DMN) during rest periods subsequent to both the HE and LE videos (Fig. 6a), consistent with functionally coherent activity within each specific network. To specifically unravel the differential connectivity during rest periods due to emotional inertia (post HE vs post LE rest periods), we directly compared the two connectivity matrices using permutation tests (see methods). Significant differences were observed for highly selective functional connections of the DMN with limbic areas: In contrast to rest periods after LE videos, rest periods after HE videos induced stronger functional coupling between the PCC and the right amygdala ($t = 1.82$, $p = 0.03$, $Z = 1.81$ one-tailed), as well as between the aMPFC and left insula ($t = 1.98$, $p = 0.02$, $Z = 2.02$ one-tailed). In addition, there was also higher coupling of the bilateral amygdala during rest periods after HE vs LE videos (right with left, $t = 1.88$, $p = 0.02$, $Z = 1.95$ one-tailed) (Fig. 6b, 6c).

Relationship between functional connectivity patterns and personality measures

Our fMRI analyses identified a selective impact of emotional videos on functional brain connectivity of the posterior part of the DMN (PCC) with the right amygdala (r.AMY) as well as of the anterior part of the DMN (aMPFC) with the left anterior Insula (l.AI) at rest, providing a plausible neural marker of emotional inertia [16,24]. To test whether these effects are related to

individual differences in socio-affective processing and personality traits, we computed a further correlation analysis between the *Z*-values from significant edges in connectivity matrices (i.e., connections between two ROIs showing a significant difference $Z > 1.64$ between post HE vs post LE rest) and specific scores on the trait anxiety (STAI-trait), rumination (RRS), and empathy (IRI). The results showed a significant positive relationship between the strength of changes in the PCC-r.AMY connectivity (rest HE – rest LE) and the individual scores of trait anxiety ($r = 0.21$, $p < 0.01$, two-tailed) and rumination ($rho = 0.22$, $p < 0.01$, two-tailed) (Fig. 7).

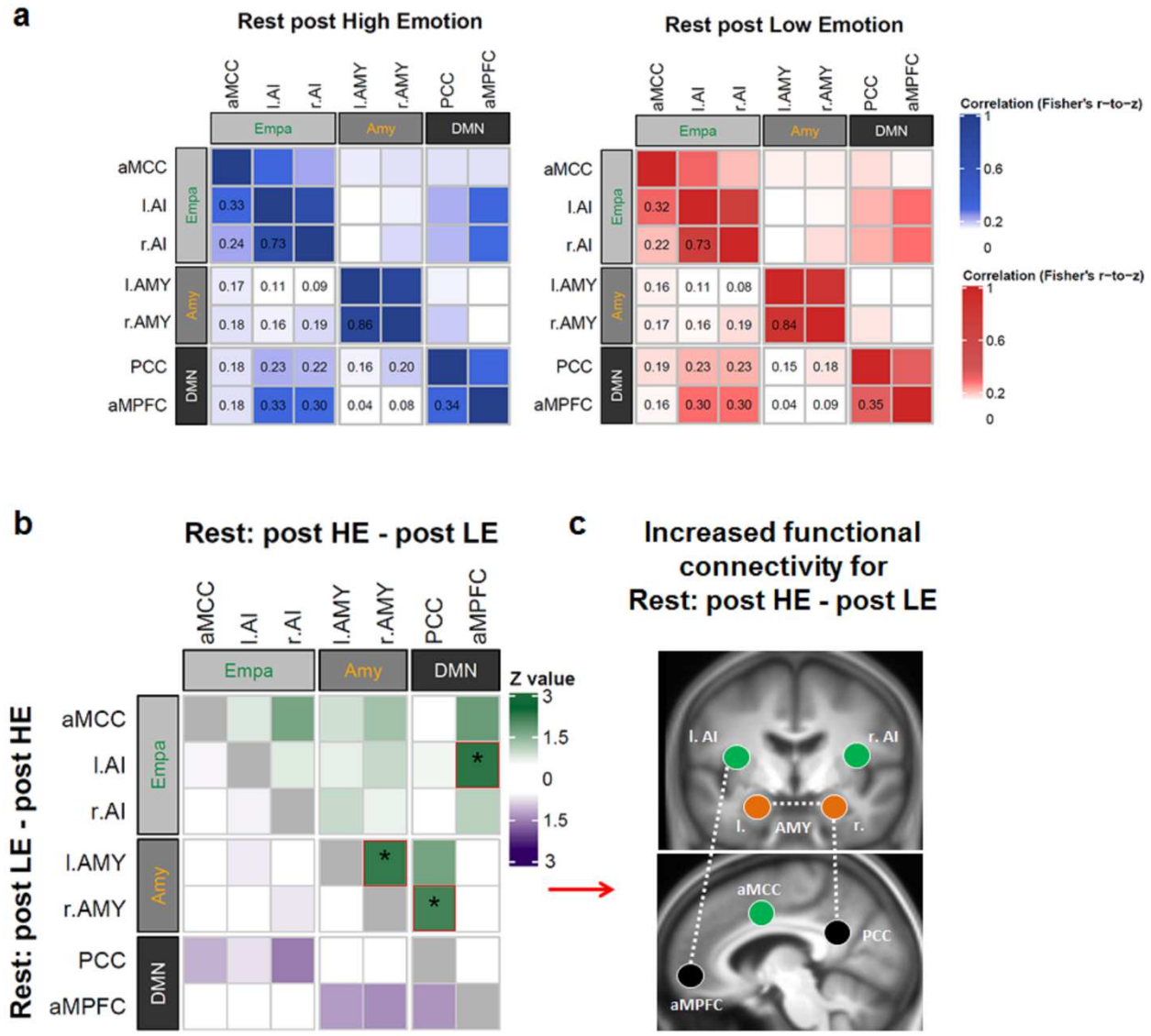

Figure 6. Functional connectivity results illustrated as (**a**) correlation matrices between pairs of ROIs for the different rest conditions. Blue matrix corresponds to post HE (high emotion) rest periods, red to post LE (low emotion) rest periods. The plotted values (correlation coefficients following Fisher's *r*-to-*z* transformation) were obtained by averaging the n = 127 correlation matrices for each condition. (**b**) Correlation matrix corresponding to the difference between the two rest conditions, showing post emotion increases (green) and post emotion decreases (violet). Left and right halves of the matrix with respect to the diagonal depict the values for inverse contrasts (upper part of the matrix: post HE - post LE rest periods; lower part of the matrix: post LE - post HE rest periods. Significant changes in correlations with $Z > 1.64$ are marked by an asterisk * corresponding to $p < 0.05$, one-tailed uncorrected). (**c**) Visual representations of significant changes in functional connections. Black ROIs= DMN regions, Orange ROIs = bilateral amygdala, Green ROIs = empathy network regions. AI: anterior insula, aMCC: anterior mid-cingulate cortex, AMY: amygdala, PCC: posterior cingulate cortex, aMPFC: anterior medial prefrontal cortex. The brain image corresponds to the average of the 127 T1 images of our sample.

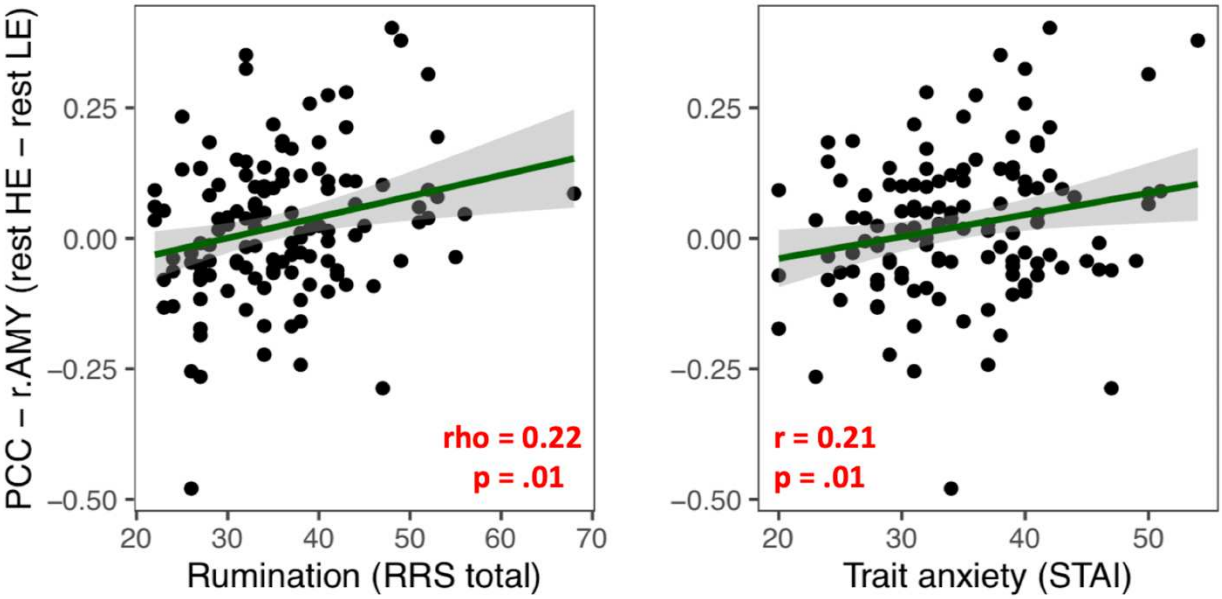

Figure 7. Pearson (*r*) and Spearman (*rho*) correlations show that higher functional connectivity between posterior cingulate cortex and amygdala during rest periods after HE > LE videos [PCC-r.AMY(rest HE-rest LE)] was positively related to trait anxiety (STAI.B) and rumination (RRS total).

Relationship between functional connectivity patterns and thought probes

Because we observed that rumination scores were positively associated with greater changes in functional coupling between PCC-r.AMY for the contrast post HE > post LE at rest, we reasoned that some participants (i.e., with higher ruminative tendencies) may have kept more negative-related content in their thoughts during the rest periods after emotional videos. This was directly tested using the explicit thought probe given after different rest conditions (see Fig. 1b). To do so, we compared the PCC-r.AMY connectivity between a subgroup of participants who verbally reported negative content in their spontaneous thoughts in response to the probe question (Present) vs. those who did not (Absent), for both the HE and LE conditions.

Behaviorally, for rest periods after HE videos, 59(54%) participants reported negative thought content, while 30(28%) reported no negative thought content and 20(18%) were ambiguous (judgments by our two raters did not match). Interrater reliability analyses revealed a good agreement (kappa=0.61) between the two independent raters (see Supplementary Table 2 for details). A Chi-square test revealed that these proportions (negative present 54% vs. negative absent 28%) were statistically different; X^2 (1, N = 109) = 45.88, p < 0.001 (two-tailed), demonstrating that HE videos induced more frequent negative than non-negative thoughts in our participants.

Conversely, for rest periods after LE videos, only 41(37%) participants reported negative thought contents, while 50(45%) reported no negative thoughts, and 19 (17%) were considered ambiguous. The rater agreement was again good (kappa = 0.66) (see Supplementary Table 2 for details). This proportion of negative thoughts (37%) was significantly lower than the proportion of non-negative thoughts (45%); Chi-squared test, X^2 (1, N = 110) = 51.59, $p < 0.001$ (two-tailed), indicating that the LE videos induced less frequent negative mental thought content (than non-negative thoughts). An additional McNemar's test further determined that, as expected, participants reported more negative thoughts for rest periods after HE videos than for rest periods after LE videos, $X^2 = 10.28$, $p = 0.02$ (two-tailed).

Finally, to relate these behavioral indices to brain effects, we used a non-parametric permutation analysis in which the PCC-r.AMY connectivity difference (*observed diff* = 0.08) between these two subgroups (negative thoughts Present-Absent) was compared to a null-distribution built by permuting the labels 5000 times. As hypothesized, we found that 54% of the participants reporting negative content in their thoughts (vs. 28% not reporting) showed increased PCC-r.AMY connectivity for the rest periods following HE videos ($p = 0.02$, one-tailed). The same difference between the two subgroups for rest periods following LE videos was only a trend (*observed diff* = 0.06; $p = 0.07$, one-tailed) (Fig. 8a,b). Taken together, these findings further unveil a direct relation between PCC-r.Amy connectivity changes after negative emotions and individual reactivity to aversive or stressful socio-emotional stimuli.

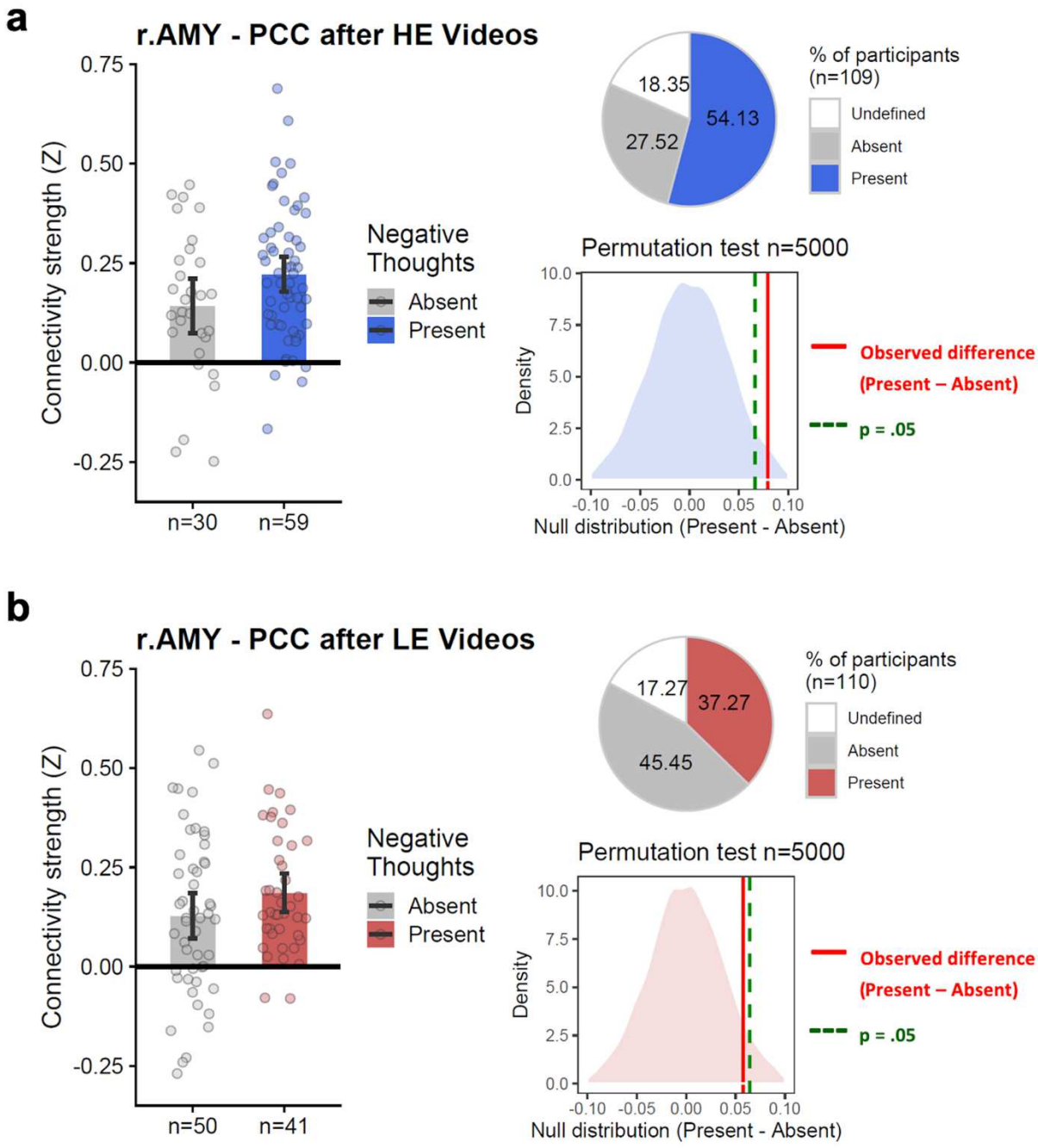

Figure 8. (**a,b**) r.AMY-PCC connectivity between the group of participants that verbally reported negative content during the thought probes (Present) vs. the group that did not (Absent), for both HE and LE conditions. After HE videos, 59(54%) participants reported negative content in their thought probes, 30(28%) did not report negative content and 20(18%) were ambiguous(undefined). After LE videos in turn, only 41(37%) reported negative content vs. 50(45)% not reporting negative thoughts and 19(17%) were ambiguous (undefined). At the brain level, the comparison was made with a non-parametric permutation analysis in which the true mean PCC-AMY connectivity difference between the groups Present-Absent (*observed diff* = 0.08) was compared to a null-distribution built by permuting the labels 5000 times. As hypothesized, we observed that 54% of the participants reporting negative content in their thoughts (vs. the 28% not reporting) showed increased PCC- r.AMY connectivity in the HE conditions (p = 0.02, one-tailed).

In the LE conditions, there was no significant difference in PCC- r.AMY connection between the two groups (*observed diff* = 0.06; p = 0.07, one-tailed). Blue: High Emotion (HE) condition, Red: Low emotion (LE) condition. r.AMY-PCC: connectivity between the right amygdala and the posterior cingulate cortex. The percentages in the text are rounded.

Discussion

The current study aimed at delineating neural markers of proficient emotional resilience and empathy in ageing, which are increasingly recognized as important protective factors against mental illness and cognitive decline in this population [71]. We assessed both reactivity and recovery of brain networks to negative socio-affective situations (i.e., during and after exposure) in a large cohort of healthy elderly, allowing us to probe for emotional carryover effects in resting state (emotional inertia) as an indicator of maladaptive regulation processes [16], and to examine their relationship with measures of anxiety, rumination, and negative thoughts.

Self-reported emotional responses to others' suffering and age-related positivity bias

Our behavioral and imaging results extend previous findings in younger adults [48]. On the behavioral level, the present data confirm that seeing others' suffering induced higher levels of negative affect, lower positive affect, and higher empathy scores than mundane scenes of daily life in the elderly, albeit at different levels (see Supplementary Fig. 3 for a comparison with young participants from Klimecki and colleagues [48]. As expected, negative affect generally correlated with higher anxiety and rumination levels in our participants (see Fig. 3c). We also found that older adults experienced positive emotions for LE more than HE videos (see Fig. 3a). Moreover, despite a restricted age range in our sample consisting solely of elderly participants (from 65 to 83 years old), we observed that the older the participants, the lower the negative and the higher the positive emotions reported to exposure of others' suffering (see Fig. 3c), consistent with the "positivity bias" often reported in the elderly [7]. This bias may reflect a motivation to upregulate positive and downregulate negative information from external emotional stimuli [7]. Here, we additionally found that this pattern was modulated by levels of empathy: higher empathy correlated not only with increased negative affect during HE videos, but also with increased positive affect during LE (see Fig. 3b). These results indicate that empathy is associated with positive emotions in older adults when confronted with social stimuli without overt emotional content, and offer a new perspective on the potential role of empathy in the "positivity bias" of older adults.

Brain activity markers of empathy in older adults

Brain responses to others' suffering (contrast HE > LE videos) implicated several regions overlapping with networks previously associated with social cognition and emotion. These encompassed regions related to the affective empathy network, pain processing, or more generally salience detection (aMCC, AI), as well as regions of the theory of mind (ToM) network (PCC, rTPJ, dMPFC), and parts of the compassion network (ventral striatum) [64,67]. These results converge with abundant work on neural activity in aMCC and AI related to empathy for pain [35,44], encoding behaviorally salient information [72,73] and negative affect [74,75]. Brain regions such as TPJ and dMPFC are engaged in scenarios requiring cognitive abilities to infer other's affective and mental state [76,77], and therefore related to cognitive aspects of empathy and theory of mind [35,66]. Interestingly, the HE>LE contrast also activated a cluster in ventral striatum, an area often associated with positive affect and reward [78] and engaged during compassion for other's suffering [56,64].

On the other hand, there was no significant activation in the amygdala during the HE > LE videos, despite its well-known role in processing emotional stimuli. This null result might accord with the notion that the amygdala responds more broadly to social or self-relevant information rather than just negative valence [79,80], and hence already activated to the content of LE videos. This would be consistent with similar increases seen during both video conditions in our study (Supplementary Fig. 1 and Fig. 5f).

Overall, our results suggest that socio-affective functions and brain regions mediating empathy and theory of mind exhibit globally normal patterns of engagement in response to complex negative social situations in healthy elderly. These data also demonstrate that our video paradigm effectively engaged emotion and empathy processes in our participants, and that healthy elderly individuals show evidence of positive affective biases in both behavioral and neural responses to social scenes, indicating preserved empathy and emotional balance in this group.

Emotional inertia and recovery from emotions after exposure to others' suffering

Beyond transient responses to negative stimuli, assessing the impact of emotions over time is crucial to determine how people cope with stressful events [81]. Emotional inertia denotes a persistence of emotional states [16] indicating inefficient recovery and greater risk for psychological maladjustment [22,81–83]. Although well-studied behaviorally [16,20], emotional inertia remains largely unexplored at the brain level, especially in old populations. To uncover its neural underpinnings, we probed for carryover effects in brain activity at rest following exposure to emotional videos.

Results revealed selective increases during rest periods after HE relative to LE videos in two major midline brain areas (ACC/MPFC and Precuneus/PCC), both constituting core parts of the

DMN typically active at rest [60], together with increases in amygdala and insula, two regions implicated in emotional processing [36]. The DMN is implicated in self-related internally-oriented processes including memory, interoception, and value-based decision making [32,33]. Interestingly, previous research found that the duration of activation in midline DMN regions was a better predictor of subjective emotional intensity of negative stimuli than the magnitude of activation [26]. A few other fMRI studies reported modulations of DMN in response to emotional challenges, although with divergent findings. While some researchers reported attenuated DMN activation following various emotions [24,25], others reported increases [26,31], similar to the current results. In the present study, we found both midline clusters of DMN (i.e., Precuneus/PCC and dMPFC) were not only activated in the HE > LE contrast during videos, but also continued their activity in the corresponding contrast during subsequent rest (post HE > post LE), providing direct evidence for "emotional inertia" in the brain.

Regarding other limbic regions, we observed that activity in the anterior insula was increased during both the (HE > LE) videos and the (post HE > post LE) rest periods, although the voxelwise activations did not fully overlap between the two conditions: while there was a more dorsal engagement during videos, more ventral parts of the anterior insula were active after the emotional event. In light of previous research in young adults [84] suggesting that dorsal AI may be recruited during adaptive behavior mechanisms while ventral AI may be highly recruited during internal homeostatic regulation, our result may reflect a shift from controlled behavioral adaptation to more spontaneous homeostatic regulation. On the other hand, although the amygdala did not differentially respond during the (HE > LE) videos, it showed a lower return to baseline levels during rest after HE vs LE videos. Accordingly, previous research showed that prolonged amygdala activity after negative images predicted greater trait neuroticism [37], and enhanced amygdala response to threat faces after negative emotion elicitation was amplified in high anxiety individuals [19].

In line with these results, our data highlight the importance of the temporal dynamics of brain responses to emotion in order to determine individual affective styles and risks for psychopathology [24,26,29].

Brain connectivity patterns related to emotional inertia

In addition, our functional connectivity analyses revealed that carryover effects in the brain were organized in two dissociable circuits, linking the posterior core of DMN in PCC with right amygdala and the anterior core in aMPFC with left anterior insula, whose respective coupling was selectively enhanced in the post HE relative to post LE rest condition (see Fig. 6). These results unveil a

"fragmentation" of the midline DMN activity and its connectivity with limbic networks induced by emotional inertia, which was accompanied by distinctive behavioral features.

The PCC and amygdala were not only more active but also functionally more connected in the post-emotional rest periods, and the strength of this enhanced connectivity was predicted by individual anxiety and rumination. Thus, participants reporting higher rumination tendencies and anxious traits on questionnaires also exhibited stronger PCC-amygdala connectivity after HE videos. Explicit verbal reports also revealed that participants expressed more negative content in the thought probe pertaining to the rest period after HE videos, and participants with more frequent negative thoughts had higher PCC-amygdala connectivity compared to those who reported no negative thoughts. This was not the case after LE videos. These findings suggest that increased functional connectivity between PCC and amygdala may directly underpin the persistence of negative content in spontaneous thoughts. Past neuroimaging research suggests that PCC is involved in internally directed cognition and memory [33] especially when people retrieve contextual and affective autobiographical information [85,86]. As the amygdala also plays a central role in affective memory by encoding and storing information about emotional relevance [34,79,87], we speculate that PCC-amygdala communication may contribute to emotional inertia and recovery from socio-emotional stressful situations, potentially by associating the content of vicarious negative experiences to personal affective memories, especially in individuals with higher levels of anxiety and rumination. These data provide new insights on neural processes associated with rumination and repetitive negative thinking, i.e., mental states implying persistent self-relevant thoughts about negative information [88] that are associated not only with maladaptive emotion regulation but also with increased risk of cognitive decline and AD [12,14]. As neurodegenerative anomalies in PCC and medial brain regions are commonly seen in AD, changes in PCC connectivity might constitute a possible neural marker for deficient affective resilience, which is in turn associated with a higher risk for dementia.

In parallel, increased functional connectivity was also observed between AI and aMPFC after HE compared to LE videos. These neural changes showed no correlation with anxiety or rumination, but only a weak positive correlation with the empathic concern IRI subscale (see Supplementary Fig. 4). These findings may reflect a more general role of AI in emotional awareness [89,90] and empathy [35], and of aMPFC in the representation of affective states in both the self and others [65,91]. These results extend prior work by showing that modulation of connectivity between these two regions may occur not only during the appraisal of socio-emotional stimuli but also persist beyond emotional events.

Limitations and future directions

Some limitations of the present study need to be acknowledged. First, while our findings extend previous work on empathy and emotional inertia that focused on young adults [24,35], we did not include a young control group for comparison. Therefore, our data do not allow us to examine any age-dependent differences. However, the current study neatly dovetails with previous findings in the younger [48,56], and provides a valuable cornerstone for future aging research. Second, we explicitly instructed our participants to watch the videos passively, and therefore some of the subsequent carryover effects on brain activity and connectivity could be interpreted as unsuccessful implicit emotion regulation styles inherent to the participants. It would be interesting to assess in future studies whether instructing participants with explicit emotion regulation strategies may change the subsequent brain response related to emotional inertia. Finally, we also acknowledge limitations related to the technical constraints of the fMRI scanner. As described in Supplementary Fig. 5, some basal forebrain voxels were automatically excluded from our group analyses due to magnetic field inhomogeneities frequently induced in brain regions near air-filled cavities in the human head [92]. Consequently, we were not able to study regions such as the orbitofrontal cortex (OFC), which plays an essential role in positive emotions and reward [56,78].

Conclusion

In conclusion, the present study demonstrates that feelings of empathy for suffering and affective resilience can reliably be investigated in the elderly using the SoVT-Rest, a novel paradigm that has very low cognitive load and high ecological validity for future applications in frail or clinical populations. Using the SoVT-Rest, we find neural and behavioral markers of the positivity bias in the elderly and show for the first time lasting carryover effects (or emotional inertia) in corticolimbic brain circuits in a population of healthy older adults. Interestingly, increased functional connectivity of PCC and amygdala during rest after high emotional events was related to anxiety, rumination, and negative thought content, making this connectivity at rest a highly likely neural substrate for emotional inertia. These findings provide an important cornerstone for better understanding empathy and emotion regulation as well as their neural signatures in the aging population and thus contribute to identifying potential risk markers for neurodegenerative diseases associated with poor stress regulation.

Data Availability

Data supporting the findings of the present manuscript are available upon request. To access to our data, please visit: https://silversantestudy.eu/2020/09/25/data-sharing/

Code availability

The code used to produce the results reported in the manuscript can be made available upon appropriate request.

References

1. Glisky, E. Changes in Cognitive Function in Human Aging. 3–20 (2007). doi:10.1201/9781420005523.sec1
2. Carstensen, L. L., Mayr, U., Pasupathi, M. & Nesselroade, J. R. Emotional experience in everyday life across the adult life span. *J. Pers. Soc. Psychol.* **79**, 644–655 (2000).
3. Mather, M. The Affective Neuroscience of Aging. (2015). doi:10.1146/annurev-psych-122414-033540
4. Reiter, A. M. F., Kanske, P., Eppinger, B. & Li, S.-C. The Aging of the Social Mind - Differential Effects on Components of Social Understanding. *Sci. Rep.* **7**, 11046 (2017).
5. Urry, H. L. & Gross, J. J. Emotion regulation in older age. *Curr. Dir. Psychol. Sci.* **19**, 352–357 (2010).
6. Lang, F. R. & Carstensen, L. L. Time counts: Future time perspective, goals, and social relationships. *Psychol. Aging* **17**, 125–139 (2002).
7. Mather, M. & Carstensen, L. L. Aging and motivated cognition: The positivity effect in attention and memory. *Trends in Cognitive Sciences* **9**, 496–502 (2005).
8. Aldao, A., Nolen-Hoeksema, S. & Schweizer, S. Emotion-regulation strategies across psychopathology: A meta-analytic review. *Clin. Psychol. Rev.* **30**, 217–237 (2010).
9. Hamilton, J. P., Farmer, M., Fogelman, P. & Gotlib, I. H. Depressive Rumination, the Default-Mode Network, and the Dark Matter of Clinical Neuroscience. *Biol. Psychiatry* **78**, 224–230 (2015).
10. Kraaij, V., Pruymboom, E. & Garnefski, N. Cognitive coping and depressive symptoms in the elderly: A longitudinal study. *Aging Ment. Heal.* **6**, 275–281 (2002).
11. Terracciano, A. *et al.* Personality and risk of Alzheimer's disease: New data and meta-analysis. *Alzheimer's Dement.* **10**, 179–186 (2014).
12. Marchant, N. L. & Howard, R. J. Cognitive debt and Alzheimer's disease. *J. Alzheimer's Dis.* **44**, 755–770 (2015).
13. Wilson, R. S., Begeny, C. T., Boyle, P. A., Schneider, J. A. & Bennett, D. A. Vulnerability to Stress, Anxiety, and Development of Dementia in Old Age. *Am. J. Geriatr. Psychiatry* **19**, 327–334 (2011).
14. Marchant, N. L. *et al.* Repetitive negative thinking is associated with amyloid, tau, and cognitive decline. *Alzheimer's Dement.* 1–11 (2020). doi:10.1002/alz.12116
15. Jané-Llopis, E. *et al. Mental Health in Older People*. (2008).
16. Kuppens, P., Allen, N. B. & Sheeber, L. B. Emotional inertia and psychological maladjustment. *Psychol. Sci.* **21**, 984–991 (2010).

17. Koval, P., Kuppens, P., Allen, N. B. & Sheeber, L. Getting stuck in depression: The roles of rumination and emotional inertia. *Cogn. Emot.* **26**, 1412–1427 (2012).
18. Van De Leemput, I. A. *et al.* Critical slowing down as early warning for the onset and termination of depression. *Proc. Natl. Acad. Sci. U. S. A.* **111**, 87–92 (2014).
19. Pichon, S., Miendlarzewska, E. A., Eryilmaz, H. & Vuilleumier, P. Cumulative activation during positive and negative events and state anxiety predicts subsequent inertia of amygdala reactivity. *Soc. Cogn. Affect. Neurosci.* **10**, 180–190 (2015).
20. Suls, J., Green, P. & Hillis, S. Emotional reactivity to everyday problems, affective inertia, and neuroticism. *Personal. Soc. Psychol. Bull.* (1998). doi:10.1177/0146167298242002
21. Koval, P., Pe, M. L., Meers, K. & Kuppens, P. Affect dynamics in relation to depressive symptoms: Variable, unstable or inert? *Emotion* **13**, 1132–1141 (2013).
22. Trull, T. J., Lane, S. P., Koval, P. & Ebner-Priemer, U. W. Affective Dynamics in Psychopathology. *Emot. Rev.* **7**, 355–361 (2015).
23. Lamke, J. P. *et al.* The impact of stimulus valence and emotion regulation on sustained brain activation: Task-rest switching in emotion. *PLoS One* **9**, (2014).
24. Eryilmaz, H., Van De Ville, D., Schwartz, S. & Vuilleumier, P. Impact of transient emotions on functional connectivity during subsequent resting state: A wavelet correlation approach. *Neuroimage* **54**, 2481–2491 (2011).
25. Pitroda, S., Angstadt, M., McCloskey, M. S., Coccaro, E. F. & Phan, K. L. Emotional experience modulates brain activity during fixation periods between tasks. *Neurosci. Lett.* **443**, 72–76 (2008).
26. Waugh, C. E., Hamilton, J. P. & Gotlib, I. H. The neural temporal dynamics of the intensity of emotional experience. *Neuroimage* **49**, 1699–1707 (2010).
27. Veer, I. M. *et al.* Beyond acute social stress: Increased functional connectivity between amygdala and cortical midline structures. *Neuroimage* **57**, 1534–1541 (2011).
28. Eryilmaz, H., Van De Ville, D., Schwartz, S. & Vuilleumier, P. Lasting impact of regret and gratification on resting brain activity and its relation to depressive traits. *J. Neurosci.* **34**, 7825–7835 (2014).
29. Waugh, C. E., Hamilton, J. P., Chen, M. C., Joormann, J. & Gotlib, I. H. Neural temporal dynamics of stress in comorbid major depressive disorder and social anxiety disorder. *Biol. Mood Anxiety Disord.* **2**, 1–15 (2012).
30. Northoff, G., Qin, P. & Nakao, T. Rest-stimulus interaction in the brain: A review. *Trends Neurosci.* **33**, 277–284 (2010).
31. Schneider, F. *et al.* The resting brain and our self: Self-relatedness modulates resting state neural activity in cortical midline structures. *Neuroscience* **157**, 120–131 (2008).
32. Raichle, M. E. *et al.* A default mode of brain function. *Proc. Natl. Acad. Sci.* (2001). doi:10.1073/pnas.98.2.676
33. Buckner, R. L., Andrews-Hanna, J. R. & Schacter, D. L. The brain's default network: Anatomy, function, and relevance to disease. *Ann. N. Y. Acad. Sci.* **1124**, 1–38 (2008).
34. LeDoux, J. The emotional brain, fear, and the amygdala. *Cellular and Molecular Neurobiology* (2003). doi:10.1023/A:1025048802629
35. Lamm, C., Decety, J. & Singer, T. Meta-analytic evidence for common and distinct neural networks associated with directly experienced pain and empathy for pain. *Neuroimage* **54**, 2492–2502 (2011).
36. Meaux, E. & Vuilleumier, P. *Emotion Perception and Elicitation*. *Brain Mapping: An Encyclopedic Reference* **3**, (Elsevier Inc., 2015).
37. Schuyler, B. S. *et al.* Temporal dynamics of emotional responding: Amygdala recovery predicts emotional traits. *Soc. Cogn. Affect. Neurosci.* **9**, 176–181 (2014).
38. Kim, M. J. *et al.* The structural and functional connectivity of the amygdala: From normal emotion to pathological anxiety. *Behav. Brain Res.* **223**, 403–410 (2011).

39. Rey, G. *et al.* Resting-state functional connectivity of emotion regulation networks in euthymic and non-euthymic bipolar disorder patients. *Eur. Psychiatry* **34**, 56–63 (2016).
40. Gross, J. J. The emerging field of emotion regulation: An integrative review. *Review of General Psychology* (1998). doi:10.1037/1089-2680.2.3.271
41. Chen, Y. C., Chen, C. C., Decety, J. & Cheng, Y. Aging is associated with changes in the neural circuits underlying empathy. *Neurobiol. Aging* **35**, 827–836 (2014).
42. Hühnel, I., Fölster, M., Werheid, K. & Hess, U. Empathic reactions of younger and older adults: No age related decline in affective responding. *J. Exp. Soc. Psychol.* **50**, 136–143 (2014).
43. Moore, R. C., Dev, S. I., Jeste, D. V., Dziobek, I. & Eyler, L. T. Distinct neural correlates of emotional and cognitive empathy in older adults. *Psychiatry Res. - Neuroimaging* **232**, 42–50 (2015).
44. Fan, Y., Duncan, N. W., de Greck, M. & Northoff, G. Is there a core neural network in empathy? An fMRI based quantitative meta-analysis. *Neurosci. Biobehav. Rev.* **35**, 903–911 (2011).
45. Krueger, K. R. *et al.* Social engagement and cognitive function in old age. *Exp. Aging Res.* **35**, 45–60 (2009).
46. MacLeod, S., Musich, S., Hawkins, K., Alsgaard, K. & Wicker, E. R. The impact of resilience among older adults. *Geriatr. Nurs. (Minneap).* **37**, 266–272 (2016).
47. Zunzunegui, M. V., Alvarado, B. E., Del Ser, T. & Otero, A. Social networks, social integration, and social engagement determine cognitive decline in community-dwelling Spanish older adults. *Journals Gerontol. - Ser. B Psychol. Sci. Soc. Sci.* (2003). doi:10.1093/geronb/58.2.S93
48. Klimecki, O. M., Leiberg, S., Lamm, C. & Singer, T. Functional neural plasticity and associated changes in positive affect after compassion training. *Cereb. Cortex* **23**, 1552–1561 (2013).
49. Poisnel, G. *et al.* The Age-Well randomized controlled trial of the Medit-Ageing European project: Effect of meditation or foreign language training on brain and mental health in older adults. *Alzheimer's Dement. Transl. Res. Clin. Interv.* **4**, 714–723 (2018).
50. Faul, F., Erdfelder, E., Lang, A.-G. & Buchner, A. G*Power 3: A flexible statistical power analysis program for the social, behavioral, and biomedical sciences. *Behav. Res. Methods* **39**, 175–191 (2007).
51. Davis, M. H. & Association, A. P. A multidimensional approach to individual differences in empathy. *JSAS Cat. Sel. Doc. Psychol.* (1980).
52. Sheikh, J. I. & Yesavage, J. A. 9/geriatric depression scale (Gds) recent evidence and development of a shorter version. *Clin. Gerontol.* (1986). doi:10.1300/J018v05n01_09
53. Spielberger, C. D., Gorsuch, R. L. & Lushene, R. State-trait anxiety inventory STAI (Form Y). *Redw. City Mind Gard.* (1983). doi:10.1515/9783111677439-035
54. Gross, J. J. & John, O. P. Individual differences in two emotion regulation processes: Implications for affect, relationships, and well-being. *J. Pers. Soc. Psychol.* **85**, 348–362 (2003).
55. Treynore, Gonzalez & Nolen-Hoeksema, S. Ruminative Responses Scale. *Cognit. Ther. Res.* (2003). doi:10.1017/CBO9781107415324.004
56. Klimecki, O. M., Leiberg, S., Ricard, M. & Singer, T. Differential pattern of functional brain plasticity after compassion and empathy training. *Soc. Cogn. Affect. Neurosci.* **9**, 873–879 (2013).
57. Benjamini, Y. & Hochberg, Y. Controlling the False Discovery Rate: A Practical and Powerful Approach to Multiple Testing. *J. R. Stat. Soc. Ser. B* (1995). doi:10.1111/j.2517-6161.1995.tb02031.x
58. Villain, N. *et al.* A simple way to improve anatomical mapping of functional brain imaging.

J. Neuroimaging **20**, 324–333 (2010).
59. Power, J. D., Barnes, K. A., Snyder, A. Z., Schlaggar, B. L. & Petersen, S. E. Spurious but systematic correlations in functional connectivity MRI networks arise from subject motion. *Neuroimage* **59**, 2142–2154 (2012).
60. Andrews-Hanna, J. R., Reidler, J. S., Sepulcre, J., Poulin, R. & Buckner, R. L. Functional-Anatomic Fractionation of the Brain's Default Network. *Neuron* **65**, 550–562 (2010).
61. Fair, D. A. *et al.* A method for using blocked and event-related fMRI data to study 'resting state' functional connectivity. *Neuroimage* **35**, 396–405 (2007).
62. Friston, K. J. Functional and effective connectivity in neuroimaging: A synthesis. *Hum. Brain Mapp.* **2**, 56–78 (1994).
63. Winkler, A. M., Ridgway, G. R., Webster, M. A., Smith, S. M. & Nichols, T. E. Permutation inference for the general linear model. *Neuroimage* **92**, 381–397 (2014).
64. Singer, T. & Klimecki, O. M. Empathy and compassion. *Curr. Biol.* **24**, R875–R878 (2014).
65. Corradi-Dell'Acqua, C., Hofstetter, C. & Vuilleumier, P. Cognitive and affective theory of mind share the same local patterns of activity in posterior temporal but not medial prefrontal cortex. *Soc. Cogn. Affect. Neurosci.* **9**, 1175–1184 (2014).
66. Schurz, M., Radua, J., Aichhorn, M., Richlan, F. & Perner, J. Fractionating theory of mind: A meta-analysis of functional brain imaging studies. *Neurosci. Biobehav. Rev.* **42**, 9–34 (2014).
67. Preckel, K., Kanske, P. & Singer, T. On the interaction of social affect and cognition: empathy, compassion and theory of mind. *Curr. Opin. Behav. Sci.* **19**, 1–6 (2018).
68. Epstein, R. & Kanwisher, N. A cortical representation the local visual environment. *Nature* (1998). doi:10.1038/33402
69. Aguirre, G. K., Detre, J. A., Alsop, D. C. & D'Esposito, M. The parahippocampus subserves topographical learning in man. *Cereb. Cortex* (1996). doi:10.1093/cercor/6.6.823
70. Boisgueheneuc, F. *et al.* Functions of the left superior frontal gyrus in humans : a lesion study. 3315–3328 (2006). doi:10.1093/brain/awl244
71. Klimecki, O. *et al.* The impact of meditation on healthy ageing — the current state of knowledge and a roadmap to future directions. *Curr. Opin. Psychol.* **28**, 223–228 (2019).
72. Seeley, W. W. *et al.* Dissociable intrinsic connectivity networks for salience processing and executive control. *J. Neurosci.* **27**, 2349–2356 (2007).
73. Menon, V. & Uddin, L. Q. Saliency, switching, attention and control: a network model of insula function. *Brain Struct. Funct.* **214**, 655–667 (2010).
74. Knutson, B., Katovich, K. & Suri, G. Inferring affect from fMRI data. *Trends Cogn. Sci.* **18**, 422–428 (2014).
75. Corradi-Dell'Acqua, C., Tusche, A., Vuilleumier, P. & Singer, T. Cross-modal representations of first-hand and vicarious pain, disgust and fairness in insular and cingulate cortex. *Nat. Commun.* **7**, (2016).
76. Bruneau, E. G., Jacoby, N. & Saxe, R. Empathic control through coordinated interaction of amygdala, theory of mind and extended pain matrix brain regions. *Neuroimage* **114**, 105–119 (2015).
77. Bruneau, E., Dufour, N. & Saxe, R. How We Know It Hurts: Item Analysis of Written Narratives Reveals Distinct Neural Responses to Others' Physical Pain and Emotional Suffering. *PLoS One* **8**, (2013).
78. Knutson, B., Fong, G. W., Adams, C. M., Varner, J. L. & Hommer, D. Dissociation of reward anticipation and outcome with event-related fMRI. *Neuroreport* **12**, 3683–3687 (2001).
79. Sander, D., Grafman, J. & Zalla, T. The Human Amygdala: An Evolved System for Relevance Detection. *Reviews in the Neurosciences* (2003).

doi:10.1515/REVNEURO.2003.14.4.303
80. Cunningham, W. A., Raye, C. L. & Johnson, M. K. 0898929042947919. 1–13 (2004).
81. Davidson, R. J. Affective Style and Affective Disorders: Perspectives from Affective Neuroscience. *Cogn. Emot.* **12**, 307–330 (1998).
82. Davidson, R. J. Well-being and affective style: Neural substrates and biobehavioural correlates. *Philos. Trans. R. Soc. B Biol. Sci.* **359**, 1395–1411 (2004).
83. Koval, P., Butler, E. A., Hollenstein, T., Lanteigne, D. & Kuppens, P. Emotion regulation and the temporal dynamics of emotions: Effects of cognitive reappraisal and expressive suppression on emotional inertia. *Cogn. Emot.* **29**, 831–851 (2015).
84. Lamm, C. & Singer, T. The role of anterior insular cortex in social emotions. *Brain Struct. Funct.* **214**, 579–591 (2010).
85. Addis, D. R., Wong, A. T. & Schacter, D. L. Remembering the past and imagining the future: Common and distinct neural substrates during event construction and elaboration. *Neuropsychologia* **45**, 1363–1377 (2007).
86. Mason, M. F. *et al.* Wandering minds: The default network and stimulus-independent thought. *Science (80-.).* **315**, 393–395 (2007).
87. Phelps, E. A. & LeDoux, J. E. Contributions of the amygdala to emotion processing: From animal models to human behavior. *Neuron* **48**, 175–187 (2005).
88. Ehring, T. & Watkins, E. R. Repetitive Negative Thinking as a Transdiagnostic Process. *Int. J. Cogn. Ther.* **1**, 192–205 (2008).
89. Critchley, H. D., Wiens, S., Rotshtein, P., Öhman, A. & Dolan, R. J. Neural systems supporting interoceptive awareness. *Nat. Neurosci.* **7**, 189–195 (2004).
90. Zaki, J., Davis, J. I. & Ochsner, K. N. Overlapping activity in anterior insula during interoception and emotional experience. *Neuroimage* **62**, 493–499 (2012).
91. Amodio, D. M. & Frith, C. D. Meeting of minds : the medial frontal cortex and social cognition. **7**, 268–277 (2006).
92. Juchem, C., Nixon, T. W., McIntyre, S., Rothman, D. L. & De Graaf, R. A. Magnetic field homogenization of the human prefrontal cortex with a set of localized electrical coils. *Magn. Reson. Med.* **63**, 171–180 (2010).

Acknowledgments

The Age-Well randomized clinical trial is part of the Medit-Ageing project and is funded through the European Union's Horizon 2020 Research and Innovation Program (grant 667696), Institut National de la Santé et de la Recherche Médicale, Région Normandie, and Fondation d'Entreprise MMA des Entrepreneurs du Futur. The authors are grateful to the Cyceron magnetic resonance imaging staff for their help with recruitment and data acquisition and administrative support and to all the participants of the study for their contribution. We acknowledge the members of the Medit-Ageing Research Group, and we thank Clara Bordas and Silvia de Cataldo for their help on the mental thoughts analyses. We are particularly grateful to Marc Heidmann for his support through different stages of this study.

Author contributions

Conceptualization: S.B.L., O.K., and P.V.; Data curation: S.B.L., Y.I.D.A., O.K., and P.V.; Formal analysis: S.B.L., and Y.I.D.A.; Funding acquisition: O.K., and P.V.; Investigation: S.B.L., and members of the Medit-Ageing Research Group; Methodology: S.B.L., O.K., and P.V.; Supervision: O.K., and P.V.; Visualization: S.B.L.; Writing – Original Draft: S.B.L.; Writing – Review and Editing: S.B.L., F.C., O.K., P.V., and Y.I.D.A.

Competing interests

The authors declare no competing interests.

Figures

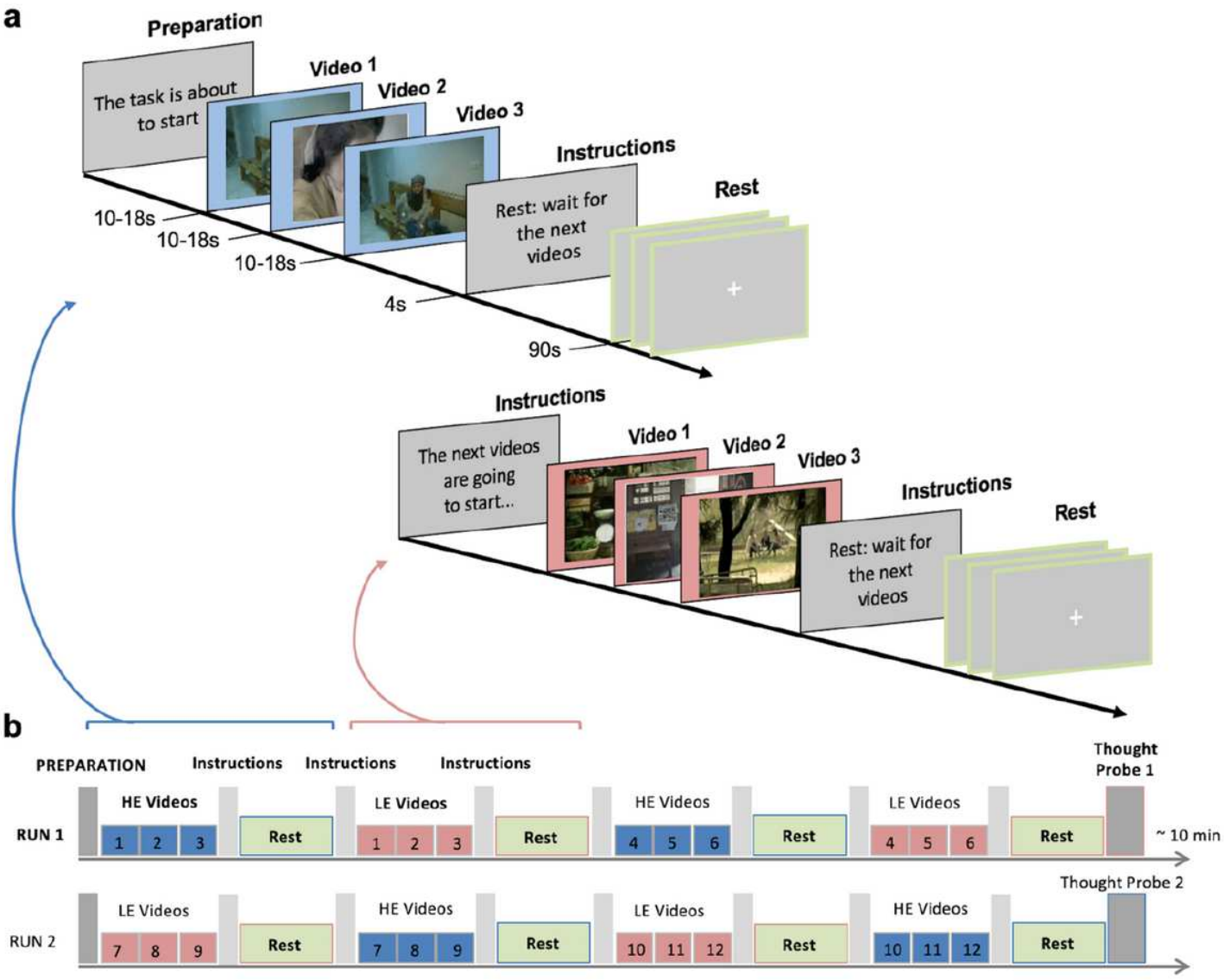

Figure 1

Experimental design: (a) SoVT-Rest paradigm: 12 High Emotion (HE) and 12 Low Emotion (LE) videos were presented grouped in blocks of three. HE videos depict suffering people (e.g., due to injuries or natural disasters), while LE videos depict people during everyday activities (e.g., walking or talking). Each block of three videos is followed by a resting state period of 90 seconds. (b) Each run ends with a thought probe in which participants verbally express what they had been thinking and/or feeling during the last rest period (via a microphone), once following a LE block and once following a HE block. The order of the runs was randomized between participants.

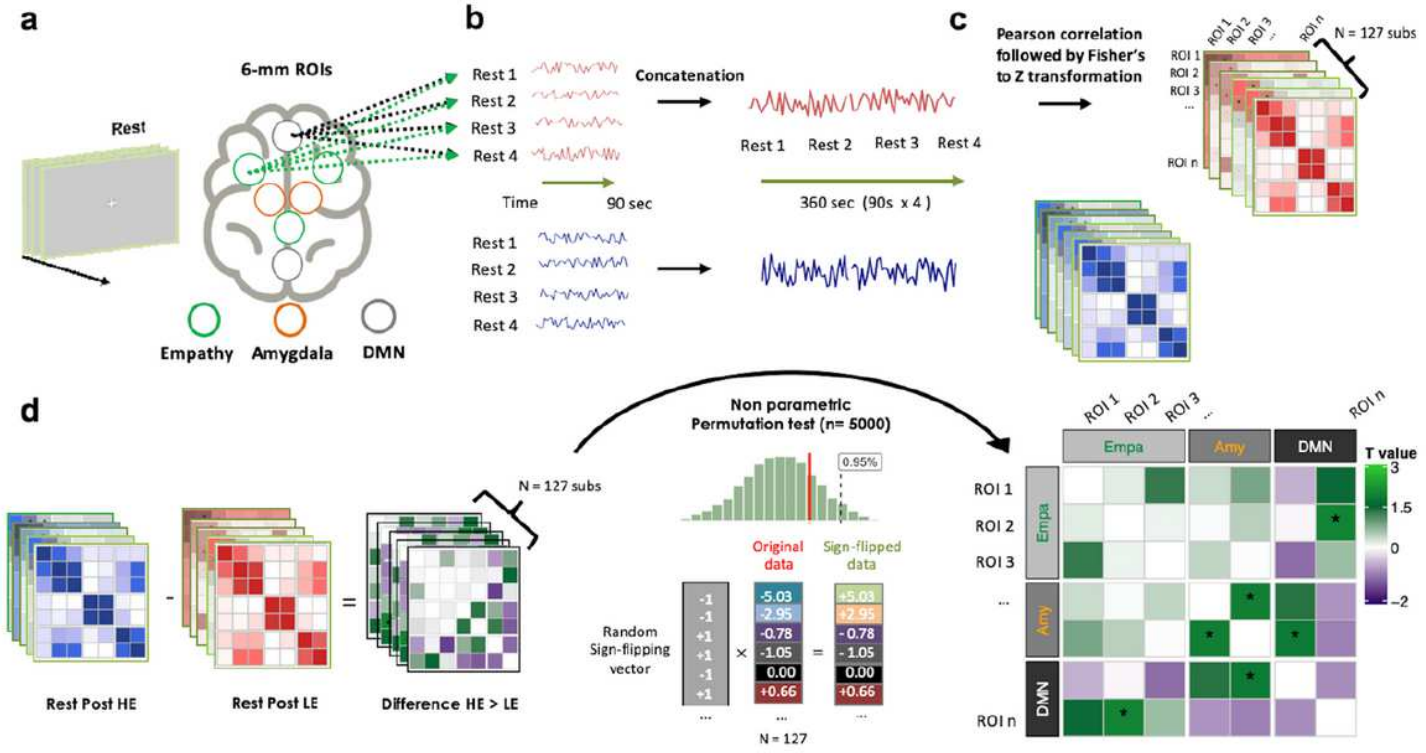

Figure 2

Functional connectivity pipeline: (a) Regions of interest (ROIs) from the default mode network (DMN) were chosen based on Andrews-Hanna et al. (2010), including the posterior cingulate cortex (PCC, - 8 -56 26) and anterior medial prefrontal cortex (aMPFC, -6 52 -2). ROIs from the empathy network were based on the meta-analysis by Fan et al. (2011), including the bilateral anterior insula (AI, -36 16 2 and 38 24 -2) and anterior mid cingulate cortex (aMCC, -2 24 38). A 6 mm-radius sphere was created for each ROI. The amygdala was defined anatomically using the SPM anatomical template. (b) For every participant, time series from the video and instruction periods were removed, and the remaining time series corresponding to the rest periods were concatenated 61. The final concatenated time series of the four rest blocks for each type of video (high emotion, HE or low emotion, LE) resulted in 184 frames (≈360 s) of resting-state data for each subject. (c) We then correlated the time-courses between the different ROIs using Pearson's r correlation, and the resulting coefficients were Fisher's r to z transformed to improve normality in the data. Individual Z-score maps (correlation matrices) were created for each participant. (d) Finally, significant differences between the two correlation matrices (post HE rest vs. post LE rest) were tested using a nonparametric permutation test 63. For each pair of nodes, the permutation test compared the true correlation difference treal (HE vs. LE) to a null distribution tpermuted constructed by randomly flipping the sign of the correlation coefficients and repeating the t statistic (n=5000).

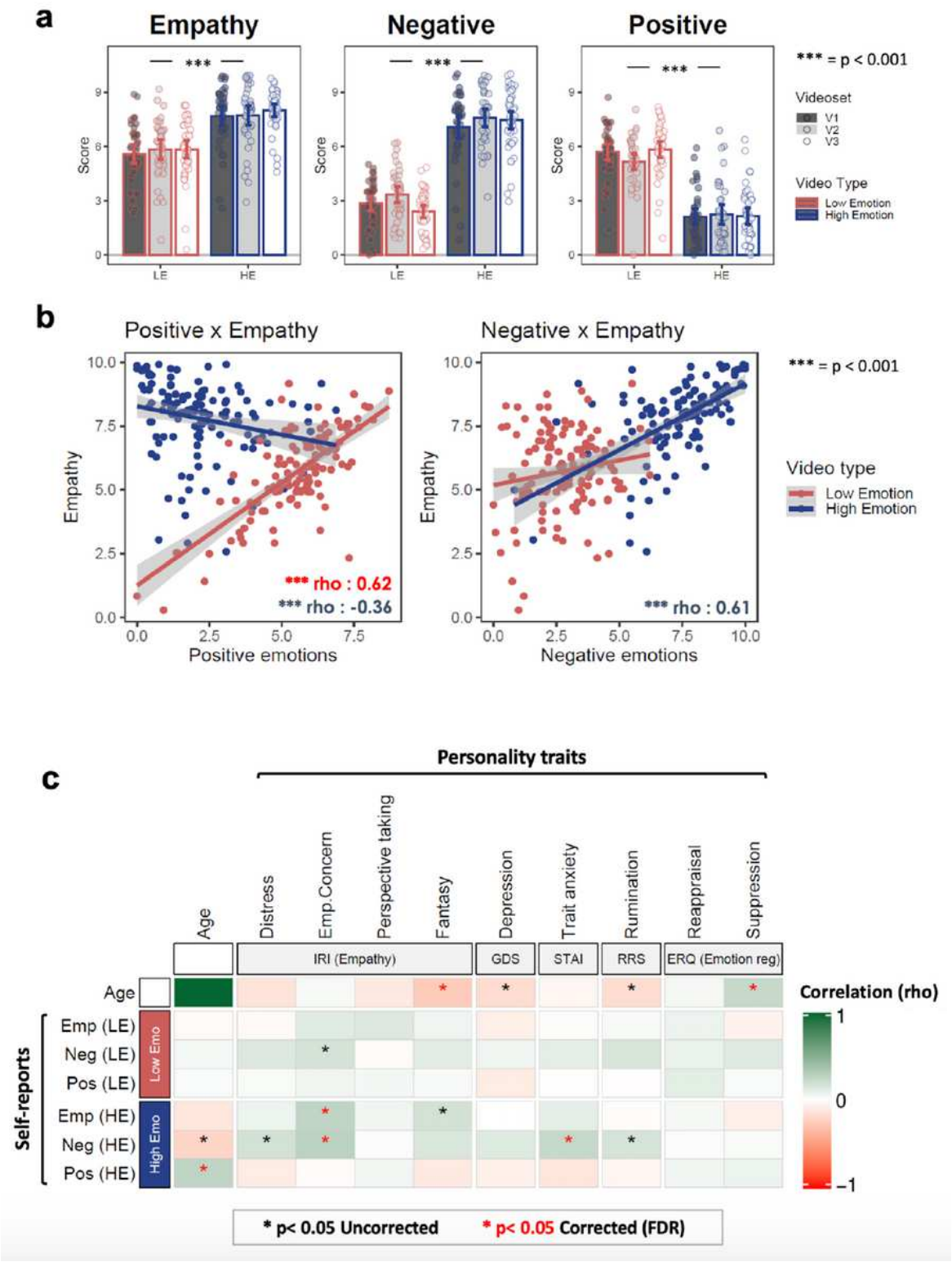

Figure 3

(a) Self-reported scores of empathy, positive affect, and negative affect for the HE and LE videos. (b) Spearman correlations between self-reported scores of empathy and affective ratings. Error bars represent 95% confidence intervals; dots represent averaged values for each participant per condition, n = 127. (c) Spearman correlations between age, personality traits, and self-reported scores of empathy, positive affect, and negative affect. Blue: HE videos, Red: LE videos, n = 126 (1 missing data point). IRI:

Interpersonal Reactivity Index, GDS: Geriatric Depression Score, STAI: STAI-trait Anxiety Index, RRS: Rumination Response Scale, ERQ: Emotion Regulation Questionnaire.

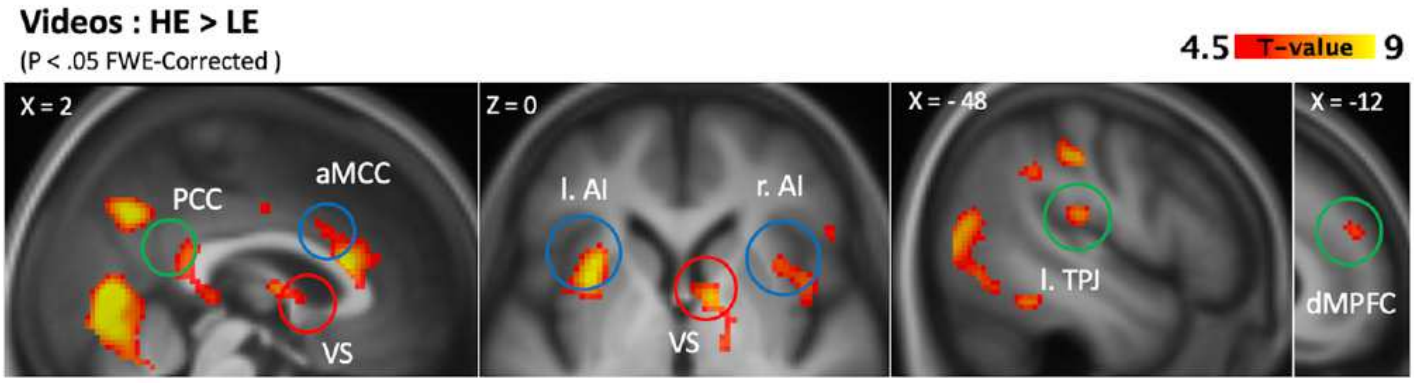

Figure 4

Brain regions with greater activation during high emotion (HE) videos in contrast to low emotion (LE) videos. Reported results are corrected for multiple comparisons using familywise error (FWE) correction at the voxel level ($p < 0.05$ FWE-corrected). Blue circles show regions previously reported as part of the Empathy network (bilateral anterior insula, AI; anterior middle cingulate cortex, aMCC), green circles show regions previously reported as part of the Theory of Mind network (PCC: posterior cingulate cortex, l. TPJ: left temporo-parietal junction, dMPFC: dorsal medial prefrontal cortex), red circles show regions associated with the Compassion network (VS: ventral striatum) 64,67. Activations are displayed on the average T1 image of our 127 participants.

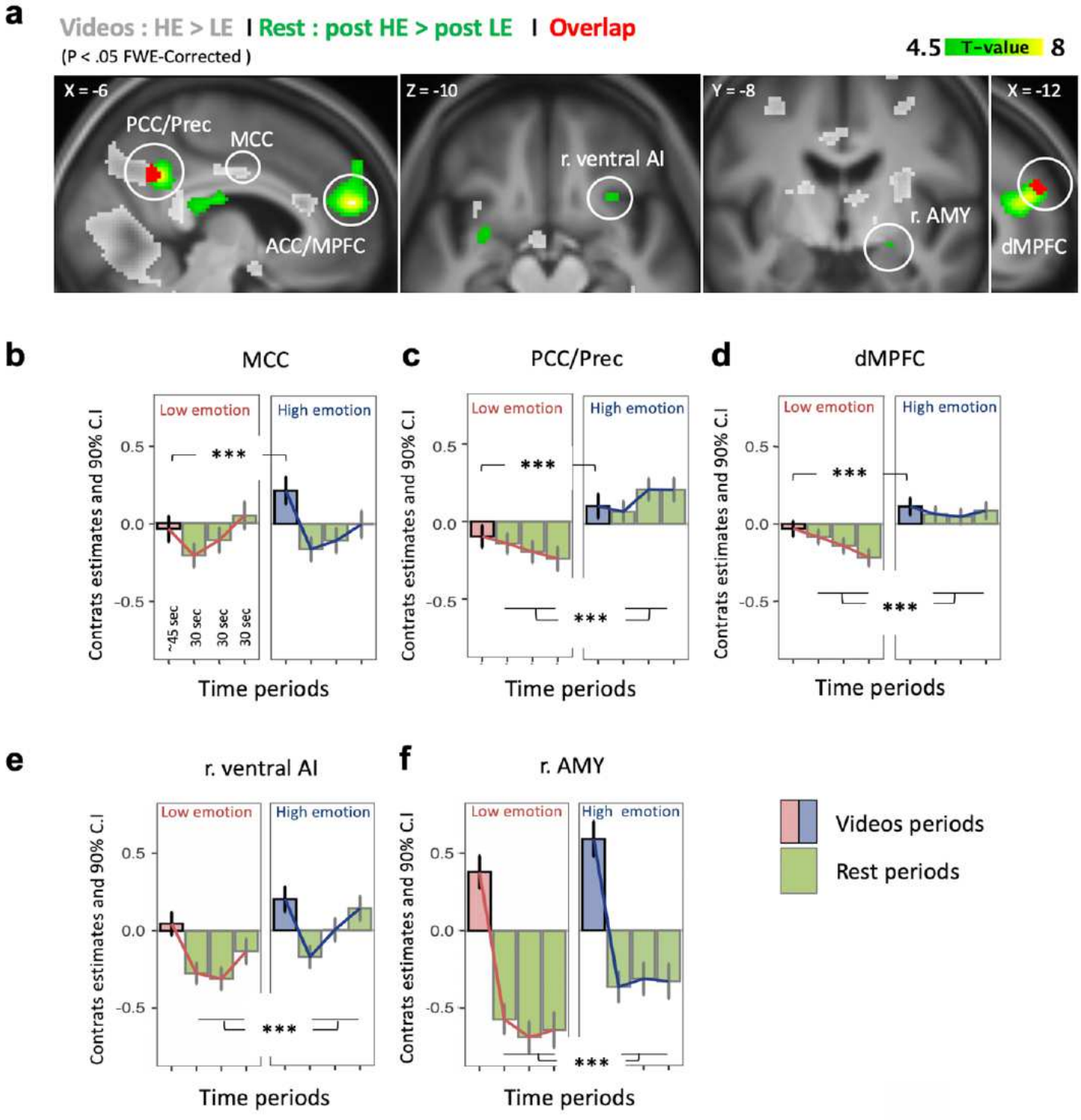

Figure 5

Brain activations to high emotion (HE) versus low emotion (LE) videos and corresponding carryover effects during rest periods. (a) Clusters in grey show brain regions significantly activated in the contrast HE videos > LE videos. Clusters in green show brain regions significantly activated in the rest periods corresponding to the contrast post HE videos > post LE videos. Red clusters show the overlap. Reported results are p < 0.05 corrected for multiple comparisons using family-wise error (FWE) correction at the

voxel level. (b,c,d,e,f) Magnitude and time-course of brain activity (parameter estimates) for relevant regions during the different task periods. (b) Example of a region (in MCC) responding to HE vs LE videos, but showing no significant difference in activation during rest after HE vs LE videos. (c,d) Example of regions (PCC/Prec and dMPFC) responding to HE > LE videos and showing significant carryover with sustained activity during subsequent rest. (e,f) The right amygdala as well as the ventral part of the right anterior insula did not reliably respond to HE vs LE videos but showed significant increases in activations during corresponding rest. Pink lines track activity time-courses during LE conditions, blue lines track activity time-courses during HE conditions. Pink and blue bars indicate activity (blocks of 3 videos = ~45 seconds) for LE and HE videos respectively, green bars indicate activity (over 3 bins of 30 seconds) during rest periods subsequent to corresponding videos periods. Activations are displayed on the average T1 image of our 127 participants. *** $p < 0.05$ FWE-corrected. PCC: posterior cingulate cortex, Prec: precuneus, MCC: midcingulate cortex, ACC: anterior cingulate cortex, MPFC: medial prefrontal cortex, dMPFC: dorsal medial prefrontal cortex, r. ventral AI: right anterior insula (ventral part), r. AMY: right amygdala.

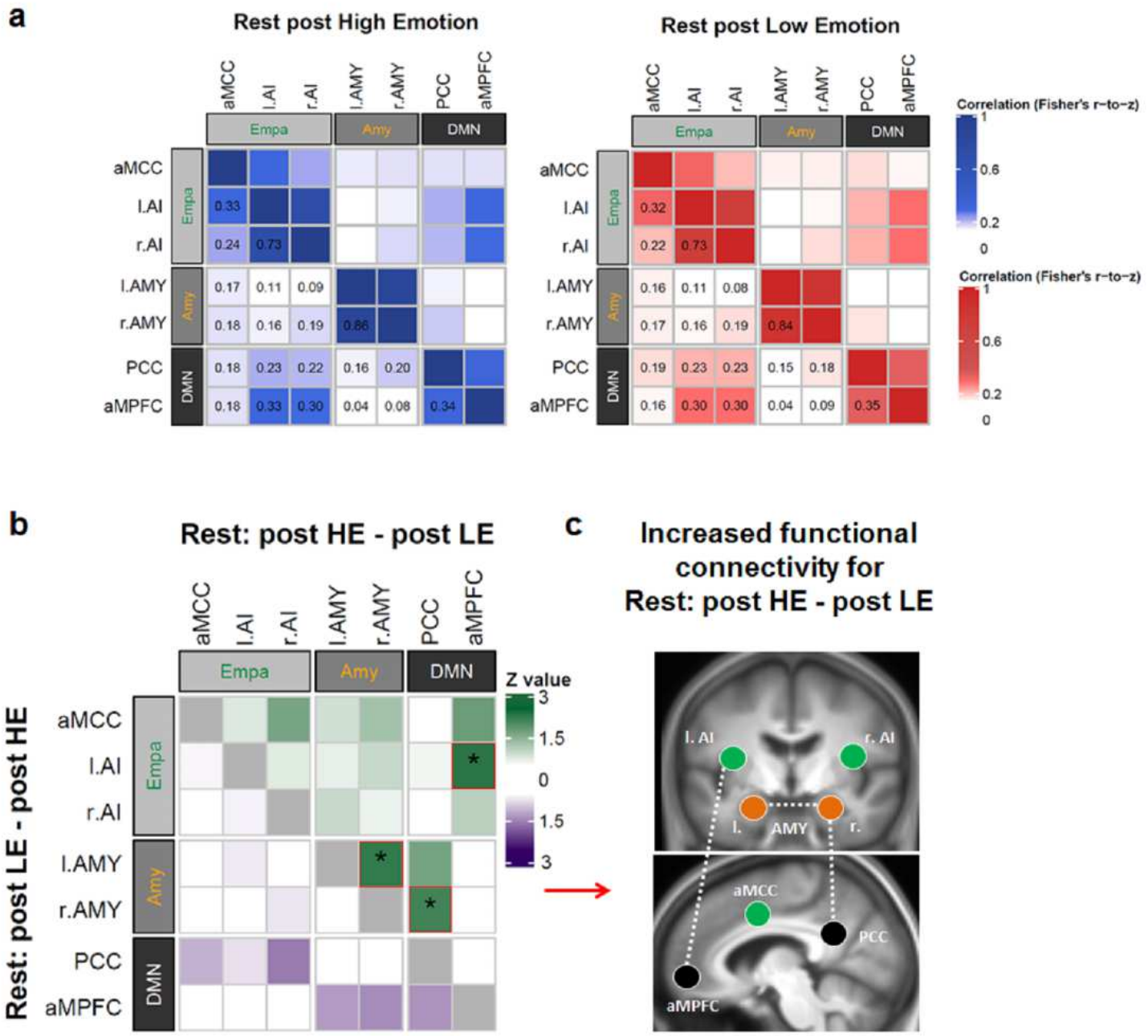

Figure 6

Functional connectivity results illustrated as (a) correlation matrices between pairs of ROIs for the different rest conditions. Blue matrix corresponds to post HE (high emotion) rest periods, red to post LE (low emotion) rest periods. The plotted values (correlation coefficients following Fisher's r-to-z transformation) were obtained by averaging the n = 127 correlation matrices for each condition. (b) Correlation matrix corresponding to the difference between the two rest conditions, showing post emotion increases (green) and post emotion decreases (violet). Left and right halves of the matrix with respect to the diagonal depict the values for inverse contrasts (upper part of the matrix: post HE - post LE rest periods; lower part of the matrix: post LE - post HE rest periods. Significant changes in correlations with Z > 1.64 are marked by an asterisk * corresponding to $p < 0.05$, one-tailed uncorrected). (c) Visual

representations of significant changes in functional connections. Black ROIs= DMN regions, Orange ROIs = bilateral amygdala, Green ROIs = empathy network regions. AI: anterior insula, aMCC: anterior mid-cingulate cortex, AMY: amygdala, PCC: posterior cingulate cortex, aMPFC: anterior medial prefrontal cortex. The brain image corresponds to the average of the 127 T1 images of our sample.

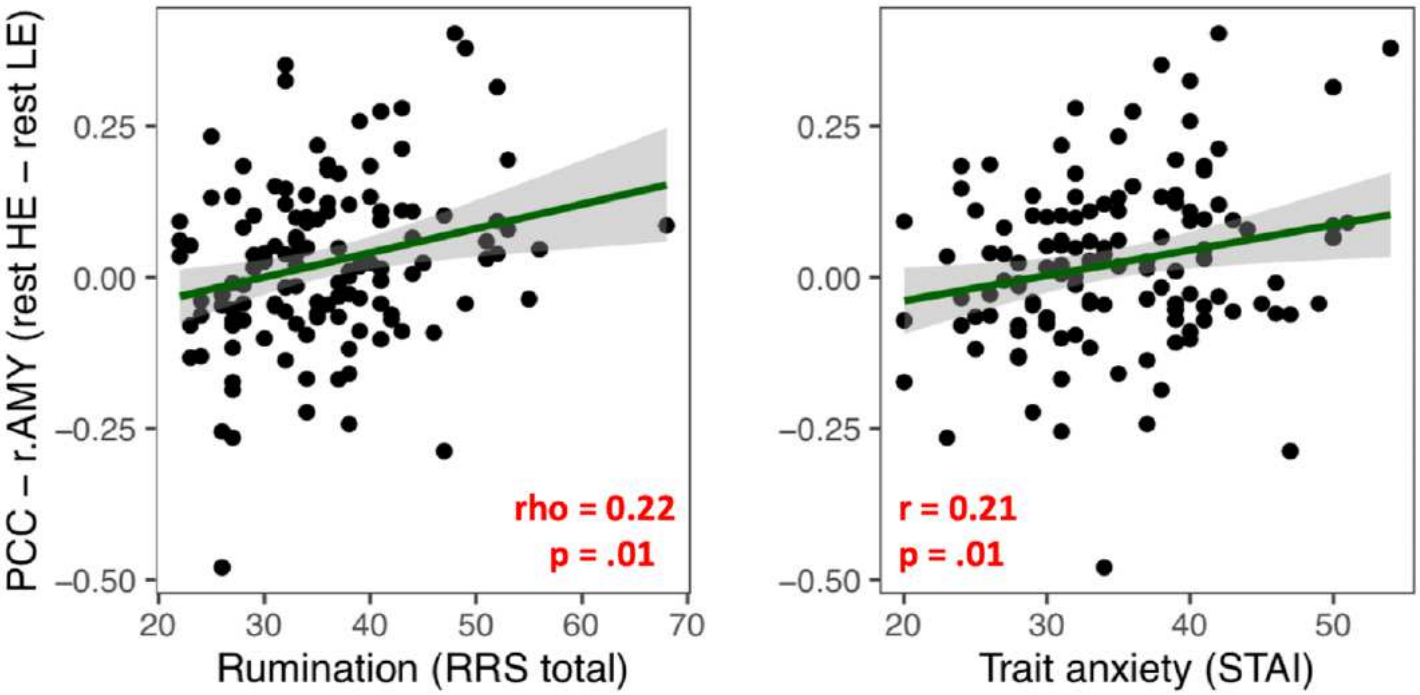

Figure 7

Pearson (r) and Spearman (rho) correlations show that higher functional connectivity between posterior cingulate cortex and amygdala during rest periods after HE > LE videos [PCC-r.AMY(rest HE-rest LE)] was positively related to trait anxiety (STAI.B) and rumination (RRS total).

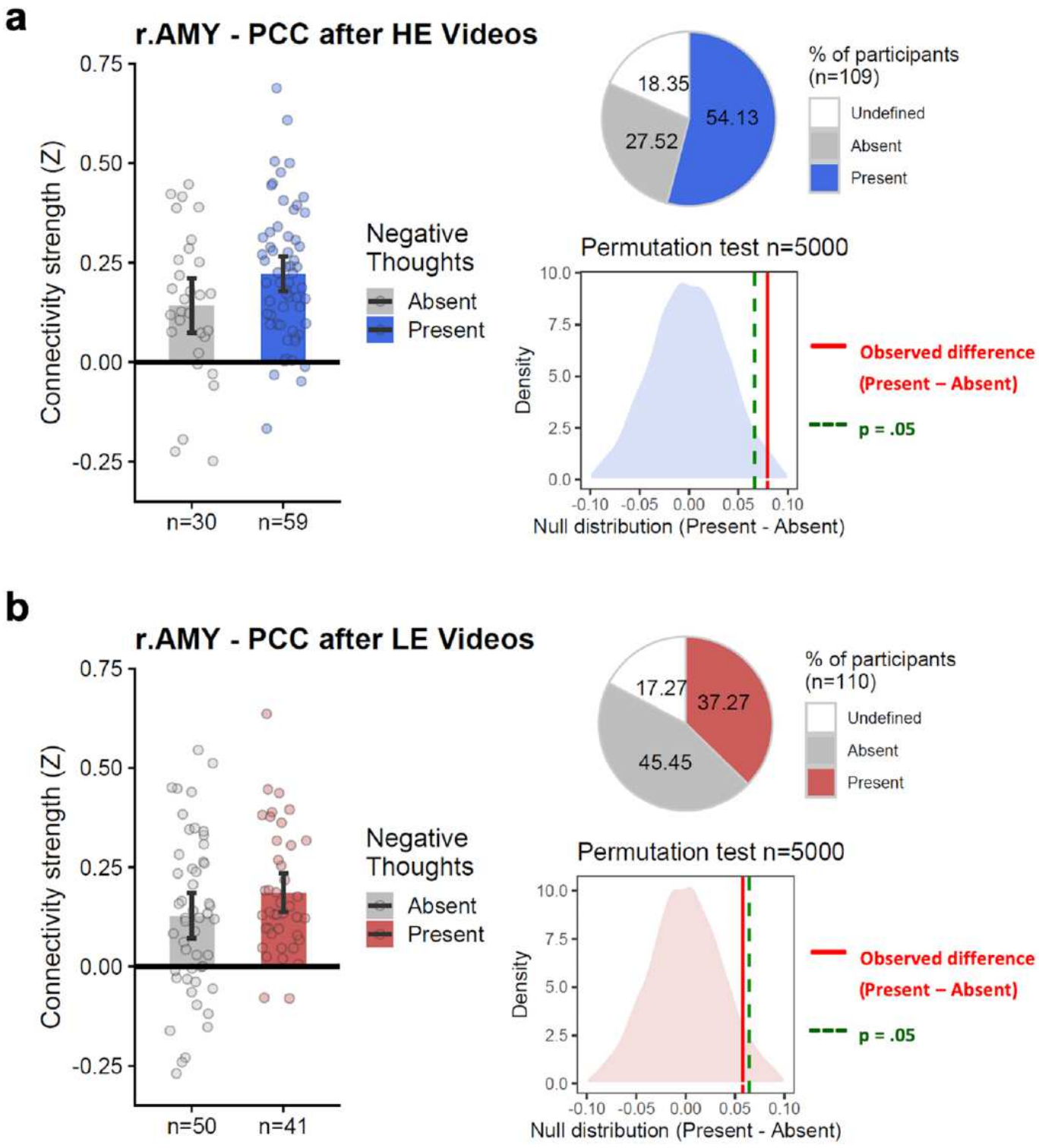

Figure 8

(a,b) r.AMY-PCC connectivity between the group of participants that verbally reported negative content during the thought probes (Present) vs. the group that did not (Absent), for both HE and LE conditions. After HE videos, 59(54%) participants reported negative content in their thought probes, 30(28%) did not report negative content and 20(18%) were ambiguous(undefined). After LE videos in turn, only 41(37%) reported negative content vs. 50(45)% not reporting negative thoughts and 19(17%) were ambiguous

(undefined). At the brain level, the comparison was made with a non-parametric permutation analysis in which the true mean PCC-AMY connectivity difference between the groups Present-Absent (observed diff = 0.08) was compared to a null-distribution built by permuting the labels 5000 times. As hypothesized, we observed that 54% of the participants reporting negative content in their thoughts (vs. the 28% not reporting) showed increased PCC- r.AMY connectivity in the HE conditions ($p = 0.02$, one-tailed). In the LE conditions, there was no significant difference in PCC- r.AMY connection between the two groups (observed diff = 0.06; $p = 0.07$, one-tailed). Blue: High Emotion (HE) condition, Red: Low emotion (LE) condition. r.AMY-PCC: connectivity between the right amygdala and the posterior cingulate cortex. The percentages in the text are rounded.

Supplementary Files

This is a list of supplementary files associated with this preprint. Click to download.

- SupplMaterialBaezLugo.pdf
- MeditAgeingResearchGroupBaezLugo.pdf